Reevaluating the Abbabis Complex: Intrusive relationships and melt connectivity in a syn-orogenic migmatite–granite system, Damara Orogen, Namibia

Thomas L. Jones[12*], A. Otto[3], E. Becker[3,4] and Andy Wilde[4]

Corresponding author: tl.jonesy8@gmail.com

[1]*School of Geosciences, University of the Witwatersrand, Johannesburg, South Africa.*

[2]*TLJ Structural Geology Consulting Ltd, Edinburgh, United Kingdom*

[3]*Deep Yellow Ltd, Subiaco, Western Australia*

[4]*Marc Geology Pty Ltd, Hillarys, Western Australia*

[5]*Boss Energy, 1/420 Hay Street, Subiaco, WA 6010, Western Australia*

Keywords: Migmatite, leucogranite, high-temperature metamorphism, partial melting, Damara Orogen, Namibia

ABSTRACT

The Abbabis Complex in the Damara Orogen has long been interpreted as a pre-Damaran (c. 1–2 Ga) basement terrane unconformably overlain by Neoproterozoic metasedimentary rocks of the Damara Supergroup. New field mapping and geochemical data from the Ida Dome and Husabberg Anticlinorium encourages re-evaluation of this interpretation. The Abbabis Complex comprises migmatites, larger leucogranite dykes and pluton-like accumulations, as well as metasedimentary rafts and schlieren. Leucogranite and migmatite bodies cross-cut overlying metasedimentary units along a gradational intrusive contact. Units mapped as "Abbabis Complex" correspond to domains where granite and migmatite become volumetrically dominant. Leucosomes of migmatites in the Abbabis Complex show similar major and trace element compositions, as well as near-identical fractionation trends, to leucogranite dykes intruding into the overlying Damara Supergroup. Leucogranite dykes are systematically more evolved, consistent with their distal location on overlying dome limbs. These relationships support field evidence that migmatites and overlying dykes formed part of an interconnected mid-crustal melt-transfer network. We interpret the Abbabis Complex in the study area predominantly as a syn-orogenic, melt-dominated migmatite–granite complex formed during high-temperature Damaran metamorphism (peaking at c. 520 Ma), involving partial melting of mainly metasedimentary protoliths and upward migration of correspondingly weakly peraluminous melt.

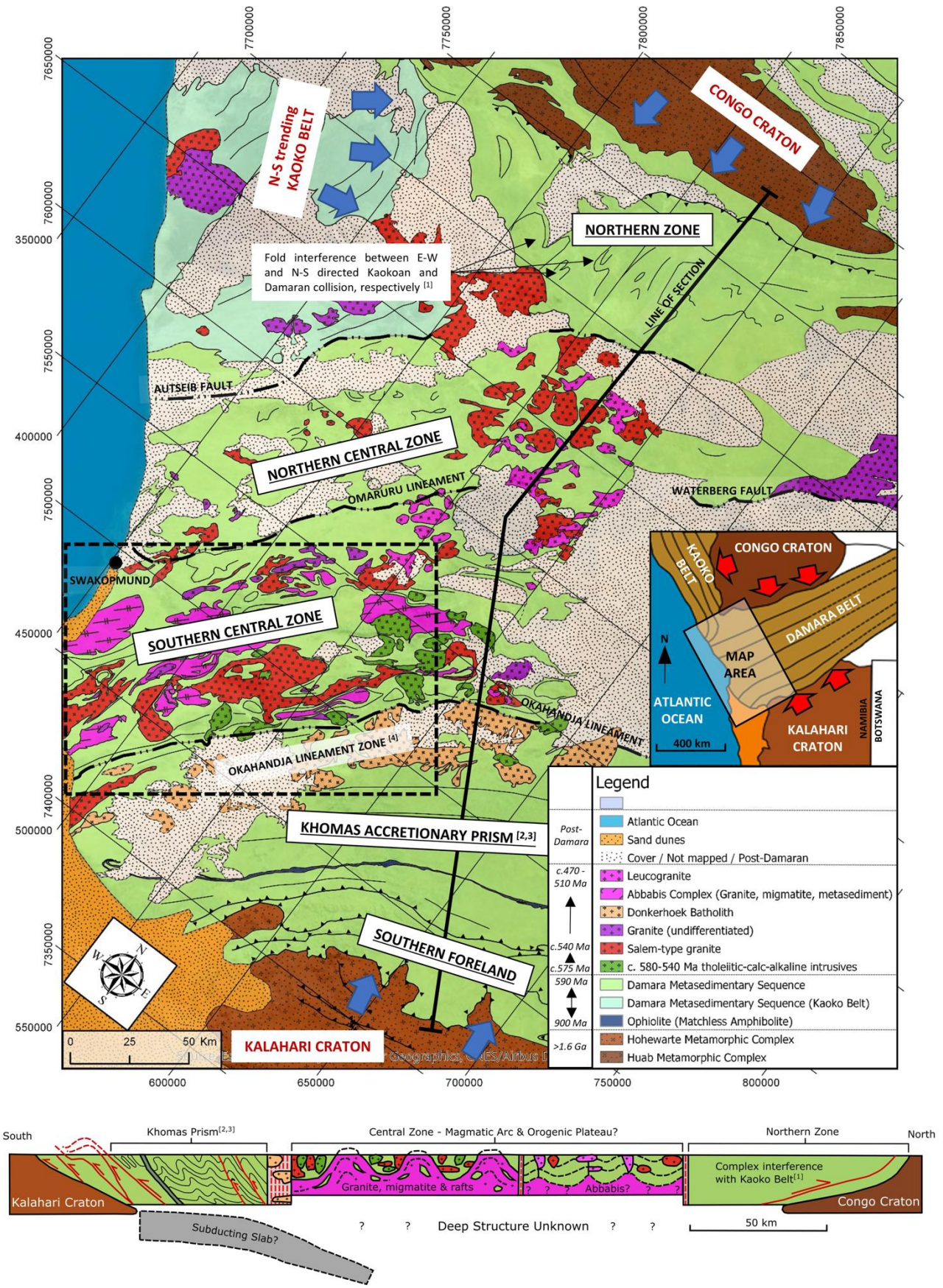

Figure 1 – Regional geological map and interpretative cross-section of the Damara Orogen, modified after Miller and Grote (1988), Geological Survey of Namibia (Sheets 2214, 2216, 2116, 2114, 2014), and Knupp (2019).

1. INTRODUCTION

Migmatite-granite complexes are fundamental components of many orogenic belts, recording partial melting, melt migration and crustal differentiation during continental collision (Weinberg & Searle, 1998; Weinberg, 1999; Searle et al., 2009; Brown, 2013). Extensive syn-orogenic partial melting and melt migration can generate melt-dominated domains that obscure earlier structural and stratigraphic relationships. In such settings, distinguishing between discrete basement terranes and syn-orogenic migmatite–granite complexes is extremely difficult, requiring careful integration of field relationships and geochronological data, along with a sound understanding of the wider tectonic setting. The Abbabis Complex in the Damara Orogen of Namibia provides a classic example of such complexity.

The Abbabis Complex outcrops at the deepest exposed level of the southern Central Zone (Figure 2) and has long been interpreted as a c. 1 or 2 Ga basement inlier upon which the Neoproterozoic Damara Metasedimentary Supergroup was deposited (Smith, 1965; Marlow, 1981; Barnes, 1981; Jacob et al., 1983; Brandt, 1987; Lehtonen et al., 1996; Longridge, 2012). The Abbabis Complex consists of 1) an older metasedimentary and metavolcanic suite, comprising marbles, quartzites, calc-silicates, schists and conglomerates, which are 2) cross-cut by a volumetrically more abundant assortment of orthogneisses, granitic gneisses, leucocratic augen gneisses and (in places) intrusive granites (Smith, 1965; Marlow, 1981; Barnes, 1981; Sawyer, 1979; Jacob et al., 1983; Brandt, 1987; Longridge, 2012). Distinguishing between pre-Damaran basement rocks and similar Damaran-aged units in the field is very difficult; Smith (1965) and Jacob et al. (1983) note general conformity of foliation between the two units, while Barnes (1981) and Longridge (2012) suggested that portions of the overlying Damara Metasedimentary Supergroup had been infolded with basement rocks during the Damara Orogeny. The modern interpretation of the Abbabis Complex as a pre-Damaran basement inlier relies heavily on geochronology. Consistent U-Pb zircon ages of c. 1 Ga and c. 2 Ga have been obtained throughout the Abbabis Complex in the southern Central Zone (Jacob et al., 1978; Kroner et al., 1991; Tack et al., 2002; Longridge, 2012; Goslin, 2019).

Many of the detailed field studies on the Abbabis Complex were undertaken several decades ago (e.g., Smith, 1965; Marlow, 1981; Sawyer, 1979; Barnes, 1981; Brandt, 1987). These studies pre-date major advances in understanding migmatites and melt migration through orogenic crust, including melt segregation at the site of partial melting, various mechanisms of melt ascent, and eventual emplacement at higher levels (see reviews by Brown, 2007; Searle et al., 2009; Brown, 2013; Cruden & Weinberg, 2018). It is also now recognized that widespread partial melting can profoundly impact the rheological

behavior of the crust, tightly coupling partial melting and melt migration to the tectonic and geodynamic evolution of orogenic belts (e.g., Jamieson and Beaumont, 2013). In highlighting these developments, we note the proposal of Toe et al. (2013), who suggested that granitic gneisses of the Abbabis Complex in the lower Swakop River may in fact represent granites and migmatites which formed from partial melting during the Damara Orogeny at c. 550-500 Ma.

This study revisits the field geology of the Abbabis Complex in two superbly exposed dome structures in the southern Central Zone of the Damara Orogen (Figure 2). Detailed field mapping, remote sensing and geochemical data are used to evaluate 1) the rock units making up the Abbabis Complex, 2) the nature of the contact between the Abbabis Complex and Damara Supergroup, 3) the genetic relationship between migmatites in the Abbabis Complex and leucogranite dykes intruding into the overlying Damara Supergroup.

GEOLOGICAL SETTING

The Damara Belt records northwest-southeast convergence between the Congo and Kalahari cratons at c. 575-500 Ma. The Damara Belt trends NE-SW across Namibia. Together with the Kaoko Belt to the north and Gariep Belt to the south (Figure 1), it forms one part of an orogenic triple junction related to collision between the Congo, Kalahari, and Rio de la Plata cratons during the amalgamation of the supercontinent Gondwana (Goscombe et al., 2017a).

The macro-scale structure of the Damara Belt consists of oppositely verging thrust wedges of the Northern and Southern zones bookending km-scale dome structures in the Central Zone (Figure 1). During collision, the Northern and Southern zones were metamorphosed at relatively low-T and high-P conditions of 8-9 kbar and 10 kbar, respectively (Goscombe et al., 2017b), while rocks in the Central Zone underwent higher-temperature / lower-pressure metamorphism.

The southern Central Zone is characterised by the highest metamorphic grade in the orogen, with regional metamorphic temperatures of ~800^{O}C and pressures of 4-5 kbar occurring at c. 520 Ma (Longridge et al., 2017; Jung et al., 2019). This high-temperature metamorphic event triggered in-situ partial melting of metasedimentary units, leading to the formation of large volumes of leucogranites in the Central Zone (e.g., Ward et al., 2008; Kisters et al., 2009; Jung et al., 2019). Leucogranites mostly have S-type signatures (Jung et al., 2001; Paul et al., 2014), although some may also have slight I-type signatures (Ashworth et al., 2020).

The stratigraphy of the southern Central Zone reportedly comprises of a Neoproterozoic Damara Metasedimentary Supergroup deposited unconformably onto Palaeoproterozoic-Mesoproterozoic Abbabis Complex basement. The lower Nosib Group of the Damara Supergroup reportedly consists of quartzites of the Etusis Formation overlain by diopside-feldspar gneiss, biotite schist and cordierite gneiss of the Khan Formation. The upper Swakop Group consists of distinctive marble-bearing sequences of the Rossing Formation, overlain by diamictite and meta-ironstone of the Chuos Formation, as well as marble of the Arandis Formation. These are overlain by thick marble and dolomite units of the Karibib Formation, as well as a thick package of pelitic schists attributed to an uppermost Kuiseb Formation (Smith, 1965; Jacob, 1974; Hoffmann et al., 2004; Miller, 2008).

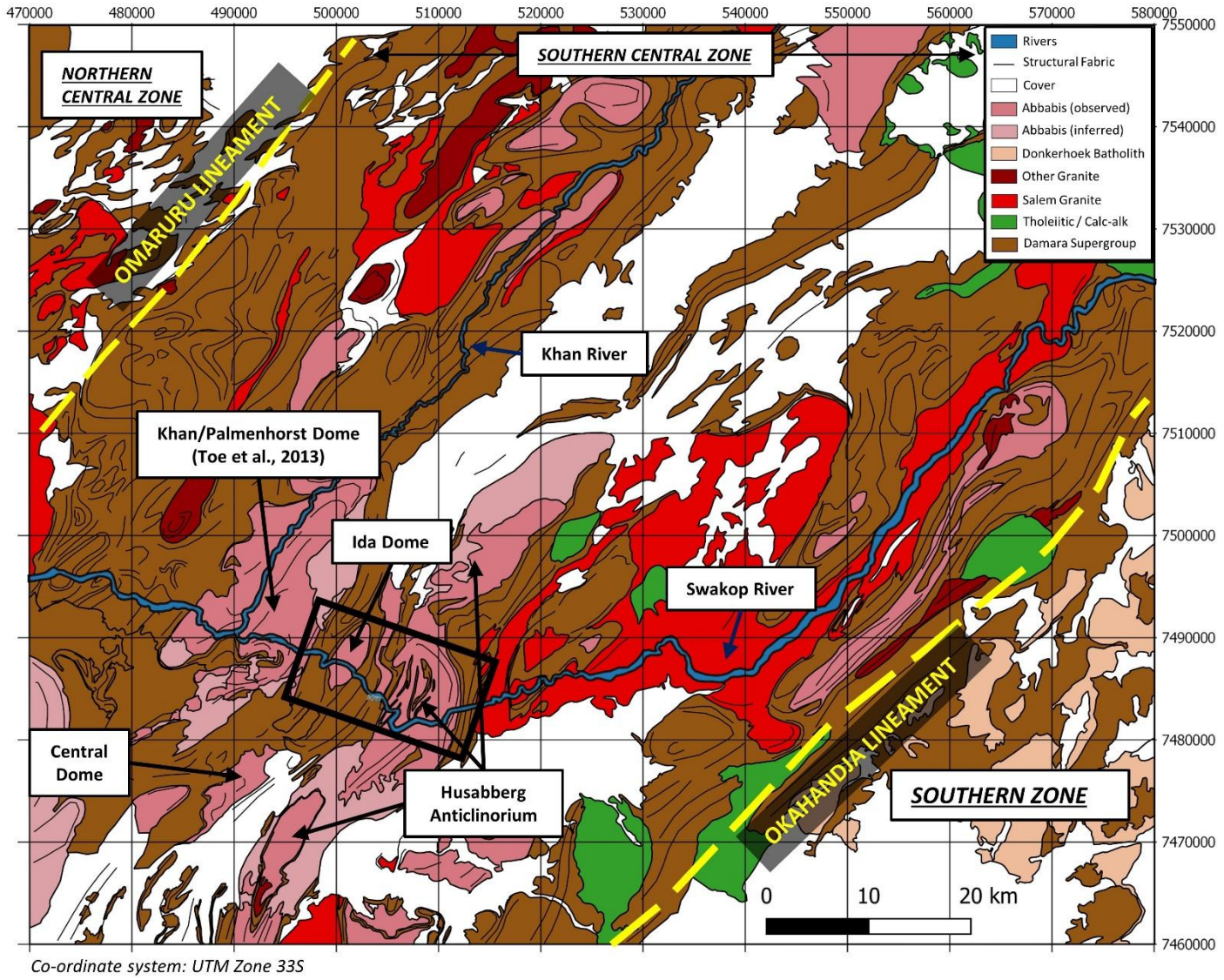

Figure 2 – Simplified geological map of the southern Central Zone in the vicinity of the Khan and Swakop rivers (modified after Geological Survey of Namibia Sheet 2214 and Knupp, 2019). Black box along the lower Swakop River outlines the study area in the Ida Dome and Husabberg Anticlinorium.

2. DATASETS & METHODOLOGY

Field mapping: New field mapping undertaken in this study focussed on the lower Swakop River section of the southern Central Zone, approximately 50 km east of the coastal town of Swakopmund (Figure 2). Detailed mapping was undertaken across two km-scale dome structures - the Ida Dome and the Husabberg Anticlinorium (Figure 5 & 6). These represent two of the largest and best exposed portions of the Abbabis Complex as they appear on existing geological maps (Figure 2; Jacob et al., 1978; Geological Survey of Namibia Map Sheet 2214). The Swakop River provides a natural geological cross-section through both dome structures with near 100% outcrop exposure.

Remote sensing: Field observations from the Swakop River were supplemented by remote sensing techniques, including airborne radiometric (Figure 3) and hyperspectral data (Figure 4), to create a detailed new geological map of the study area (Figure 5). The locations of key features and field photos discussed in text below (Figure 7 to 15) are shown on the geological map in Figure 5, as well as a schematic cross-section (Figure 6) which summarises key geological observations made along the river gorge.

Geochemistry: The location of rock samples collected for geochemical analysis are shown in Figure 5. Eight samples of granitic leucosome were collected from migmatites of the Abbabis Complex in the core of the Ida Dome, as well as 12 samples of leucogranite dykes intruding into the overlying Damara Supergroup on the dome limbs (Figure 5). Samples were submitted to ALS Laboratories in Okahandja, Namibia, for analysis in Perth, Western Australia. Samples were crushed and pulverized to 85% passing 75 µm. Major element oxides were determined using the ALS ME-ICP06 whole-rock package following lithium borate fusion, with concentrations measured by inductively coupled plasma–atomic emission spectrometry (ICP-AES). Trace elements were analysed using lithium borate fusion with inductively coupled plasma–mass spectrometry (ICP-MS; method ME-MS81). Loss on ignition (LOI) was determined by thermogravimetric analysis (TGA furnace; method ME-GRA05). Selected base metals were analysed following four-acid digestion (ME-4ACD81). Analytical precision and accuracy were monitored using internal standards and quality control procedures implemented by ALS.

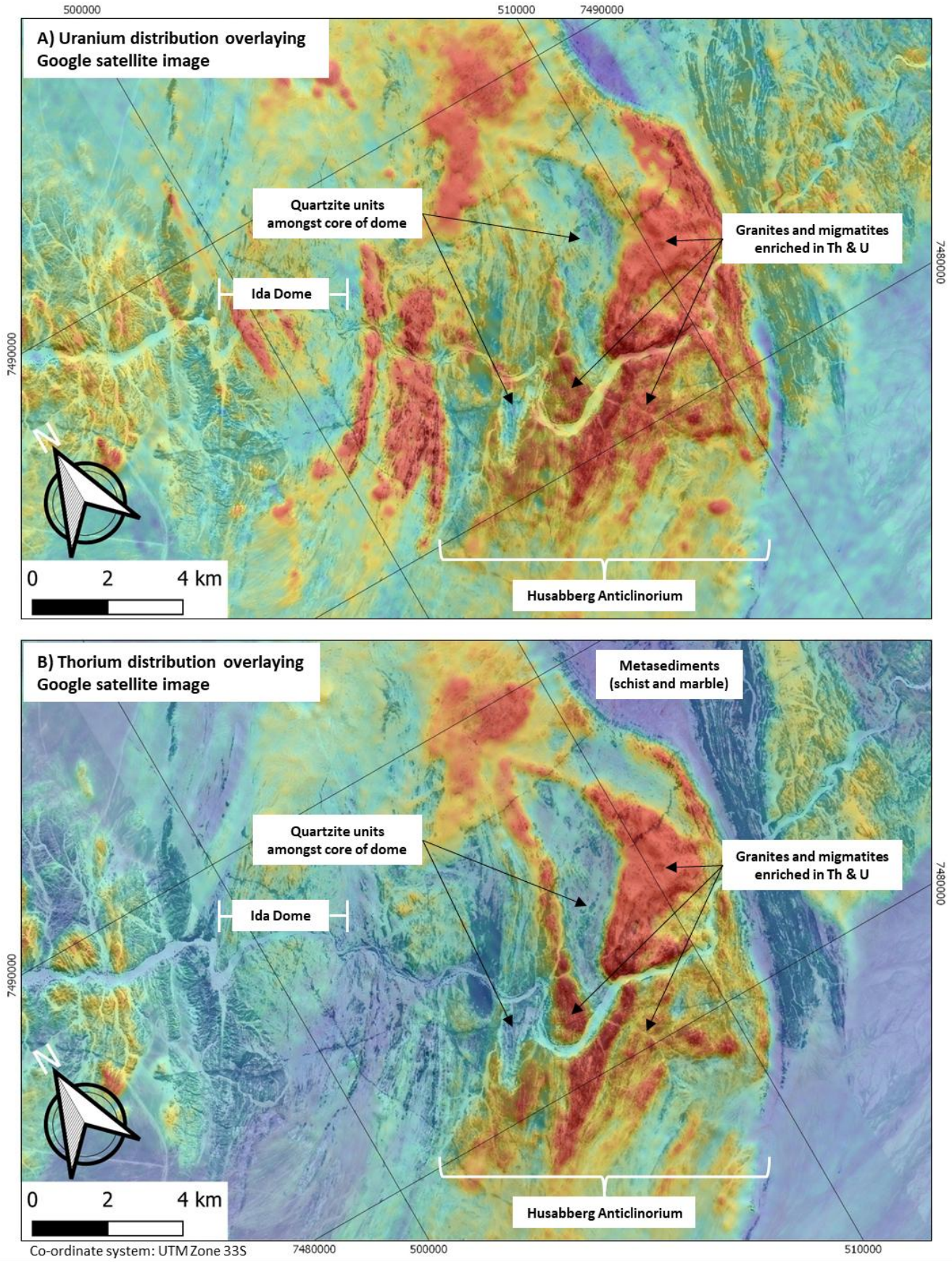

Figure 3 – Airborne radiometric dataset showing the distribution of A) uranium and B) thorium in different rock units at the Ida Dome and Husabberg Anticlinorium. Data flown on behalf of the Geological Survey of Namibia.

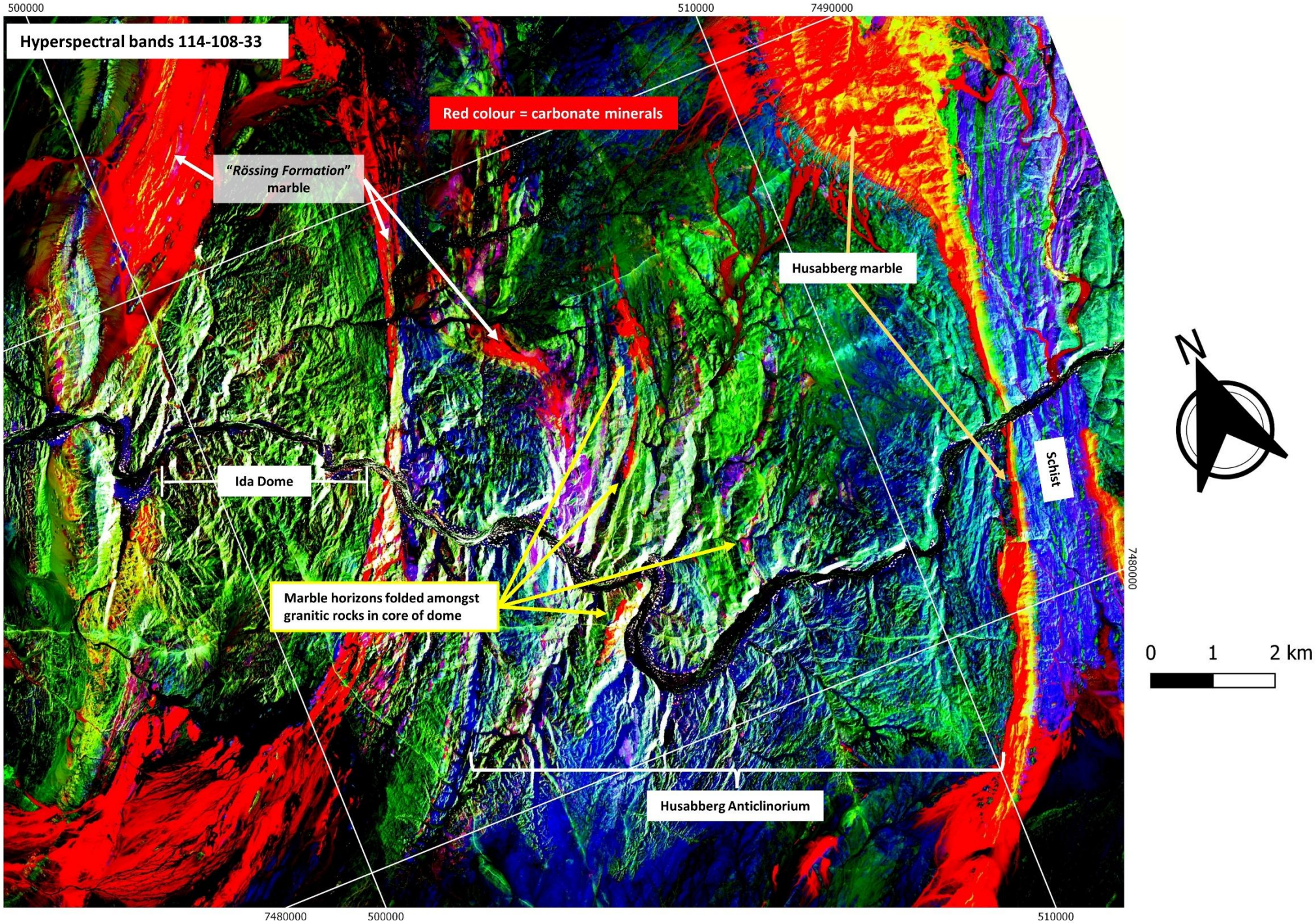

Figure 4 – Example of hyperspectral data (band ratio 114-108-33) used to interpret the geology in the vicinity of the Swakop River. For interpretation see corresponding geological map in Figure 5.

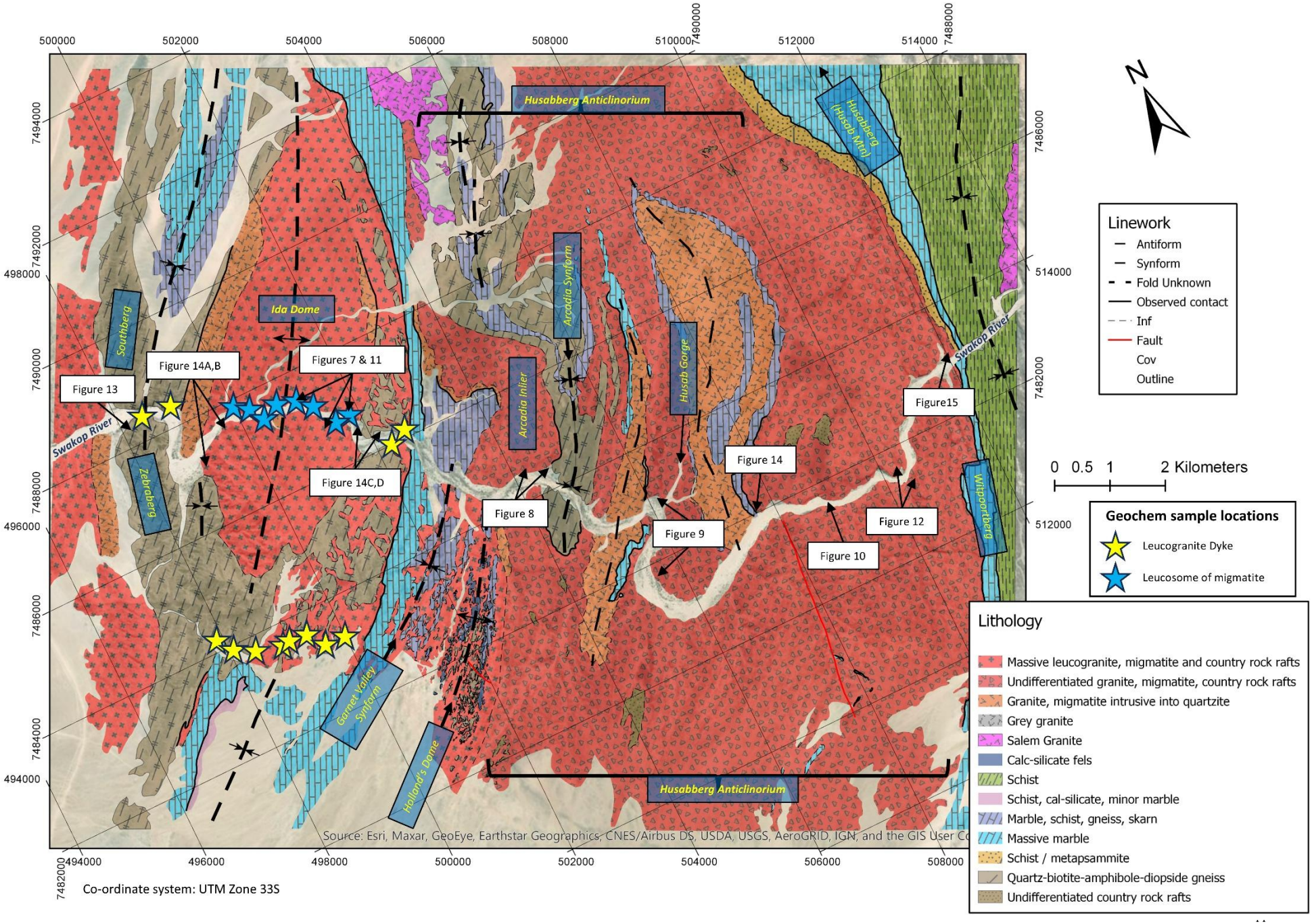

Figure 5 – Interpreted geological map of the Ida Dome and Husabberg Anticlinorium. Modified from previous maps (Barnes, 1981; Corvino and Pretorius, 2013; Kruger and Kisters, 2016; Knupp, 2019) using airborne radiometric and hyperspectral data alongside extensive new field observations.

fd

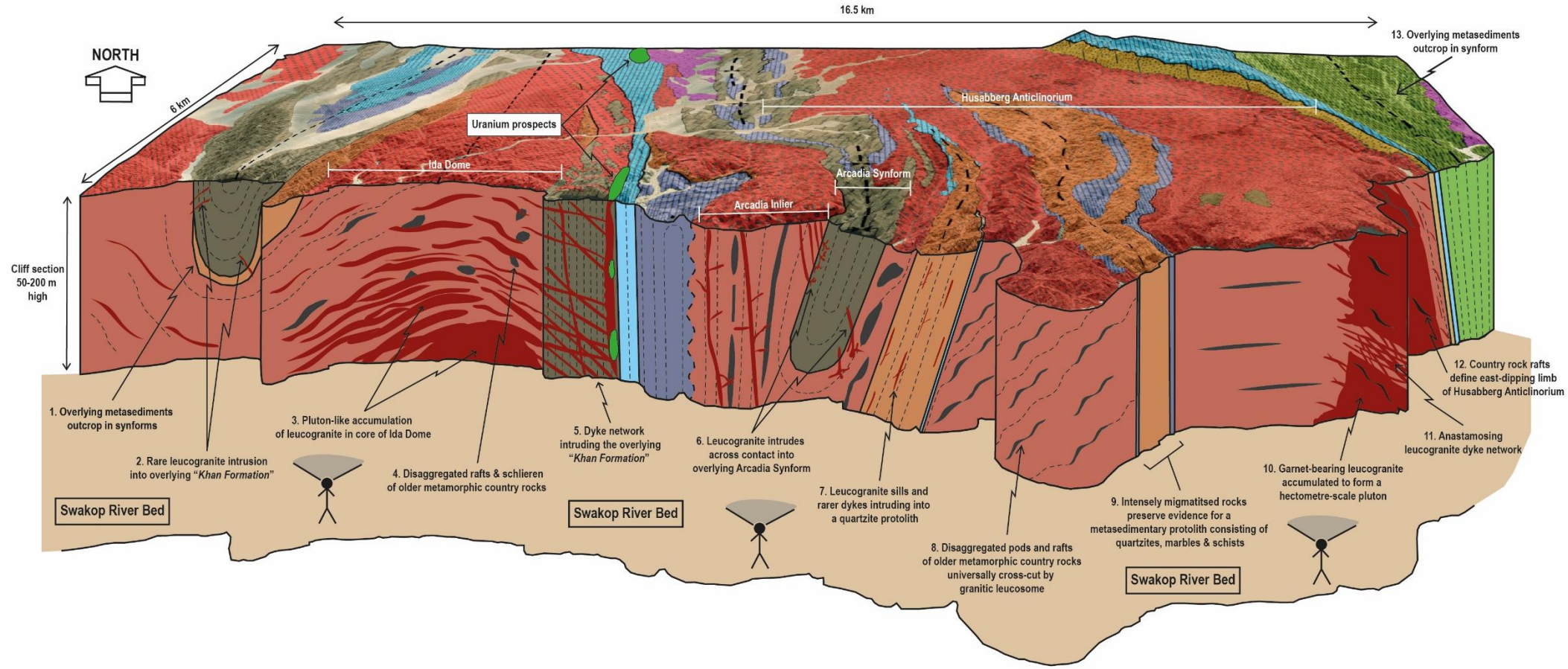

Figure 6 – Schematic 3D block diagram illustrating key field relationships observed along the lower Swakop River. For interpretation of the rock units see the corresponding geological map in Figure 5.

3. RESULTS

3.1 Field geology: Abbabis Complex

3.1.1 Metatexite and diatexite migmatites

At the Ida Dome, the proportion of granite increases with depth. Metatexite migmatites grade into diatexite migmatites at deeper structural levels. Migmatites show patch, stromatic, and net-like textures (Figure 7A). Stromatic leucosomes merge seamlessly with leucosome bodies in cross-cutting shear bands (Figure 7C). Foliation-parallel leucosomes merge with cross-cutting dyke-like structures (Figure 7D). Many migmatites display complex outcrop patterns, with cm-scale folds locally cross-cut by larger leucogranite bands (e.g., Figure 7E).

At the Arcadia Inlier, on the western edge of the Husabberg Anticlinorium (Figure 5 & 6), approximately 65-80% of the outcrop area consists of a stromatic migmatite, with subordinate leucogranite dykes (20-30% of outcrop area) and rare pods and rafts of older quartz-amphibole-biotite gneiss (Figure 8). Pinch-and-swell leucosomes in the migmatite locally merge seamlessly with the larger leucogranite dykes (Figure 8B and 8C).

In the western portion of the Husabberg Ancticlinorium, the Abbabis Complex is dominated by a variety of metatexite and diatexite migmatites. In the vicinity of the Husab Gorge (Figure 5), rocks form an ~1 km thick body of stromatic diatexite migmatites. Distinctive garnet crystals occur in association with patch migmatites, where the leucocratic component is diffuse and distributed throughout the host country rock (Figure 9A). Stromatic leucosomes lead away from the patch migmatites and merge seamlessly with larger leucogranite dykes cutting across the foliation (Figure 9B). The bulk of granitic leucosome forms thin bodies oriented parallel to the foliation in the country rock gneisses.

The remainder of the Husabberg Anticlinorium, east of a distinctive quartzite unit (Figure 5&6), consists of a vast accumulation of diatexite migmatite (Figure 10). These diatexite migmatites correspond to the “red granite gneiss” mapped by Jacob (1974). These migmatites are primarily stromatic. Net-textured migmatites are also locally observed where transgressive granite bodies merge with stromatic foliation-parallel leucosomes (Figure 10D). Many migmatites have been deformed into L>S tectonites;

when observed in cross-section, they locally resemble the augen gneisses described by Jacob (1974) and Barnes (1981).

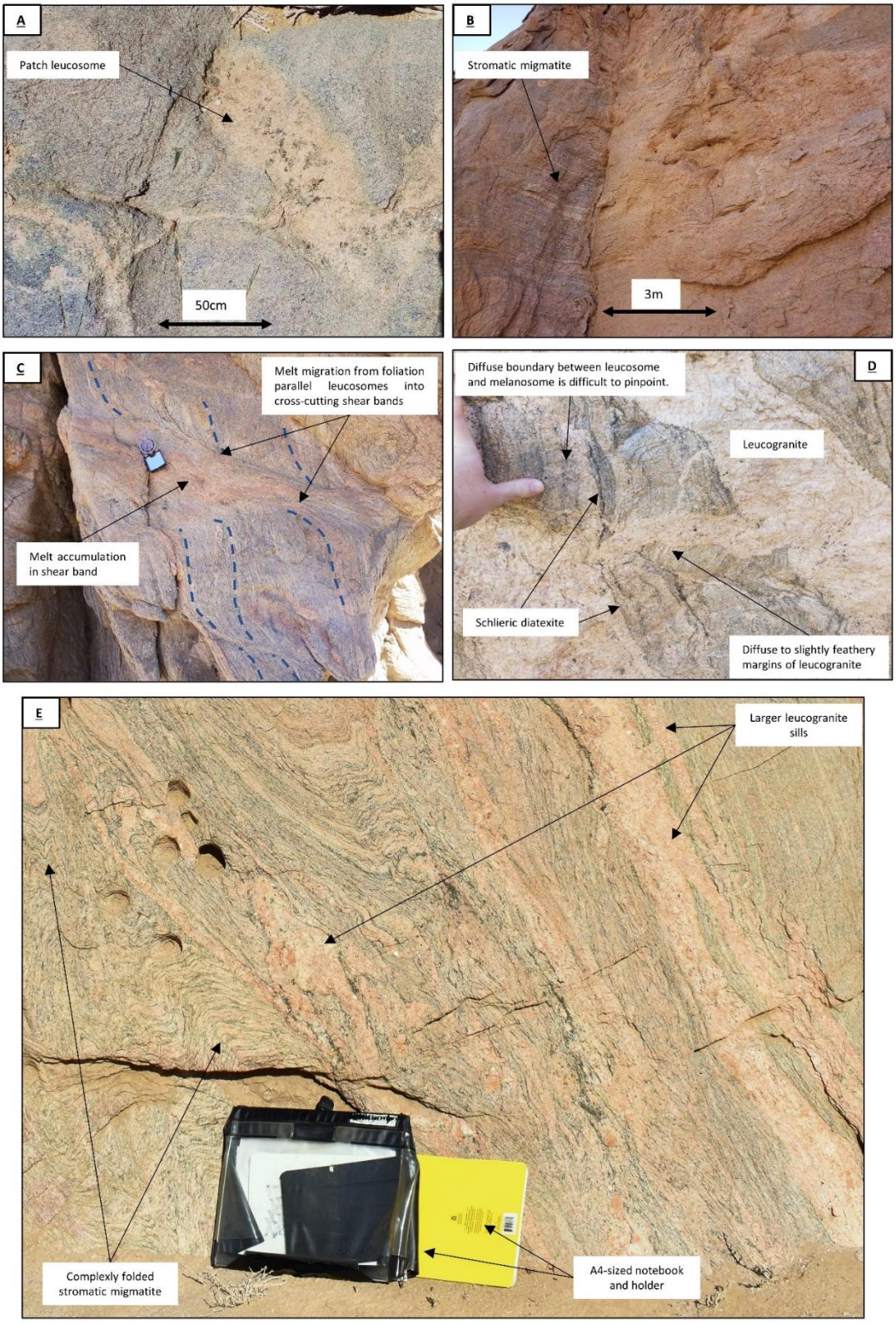

Figure 7 – Migmatites in the core of the Ida Dome. A) Patch migmatite; B) Stromatic migmatite; C) Net-textured migmatite D) Cross-cutting dyke-like structure with locally diffuse & feathery margins; E) Complex migmatite outcrop patterns .

1

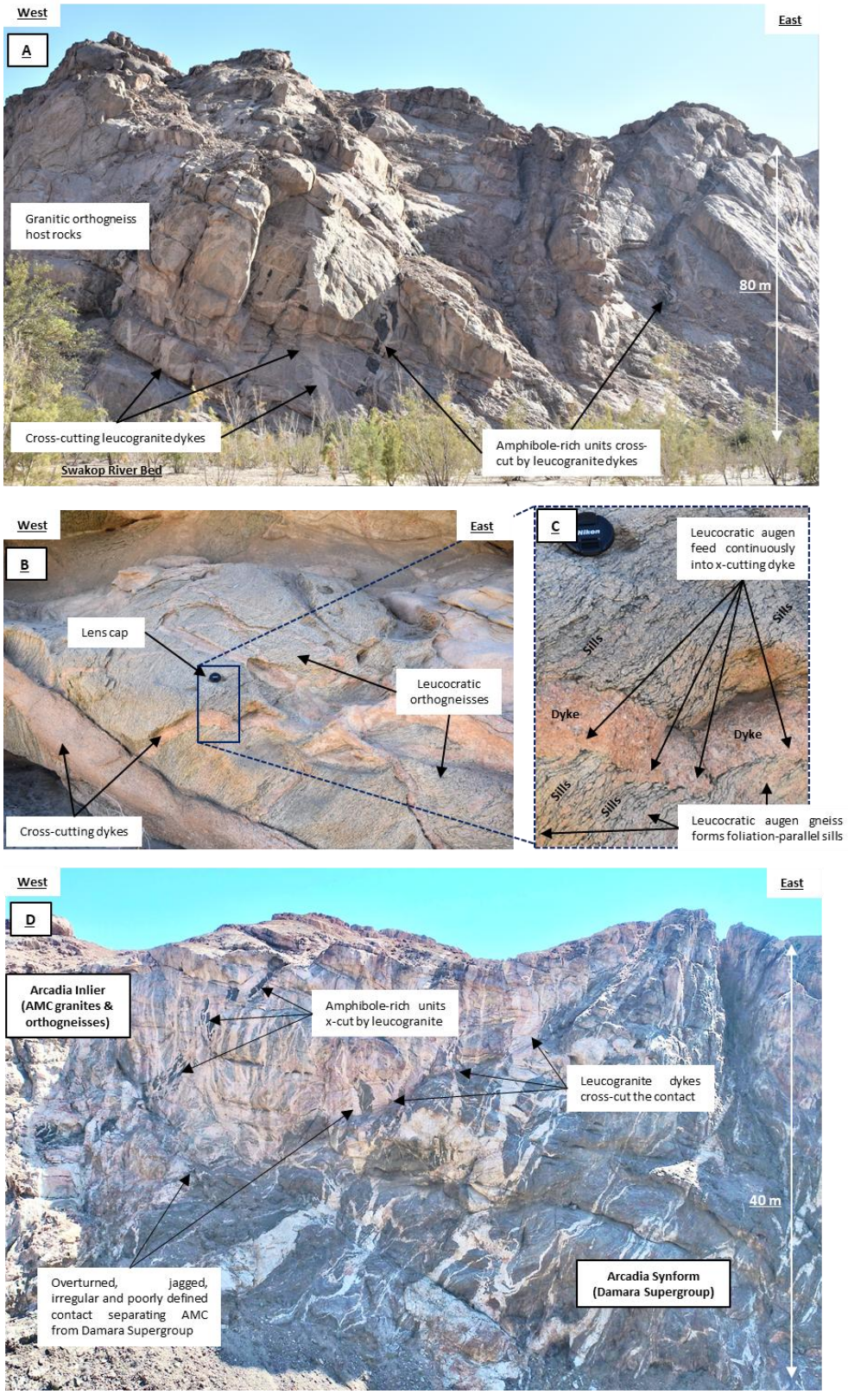

Figure 8 – Abbabis Complex at the Arcadia Inlier. A) Migmatites and amphibole-rich units transgressed by leucogranite dykes. B) Close-up of [A]. C) Close up of [B] showing petrographic continuity between leucosomes and larger dyke-like structures. D) Overturned contact between the Abbabis Complex and the "Khan Formation" of the Damara Supergroup – note the absence of the "Etusis Formation", as well as leucogranite dykes intruding across the contact and into the metasediments of the Damara Supergroup.

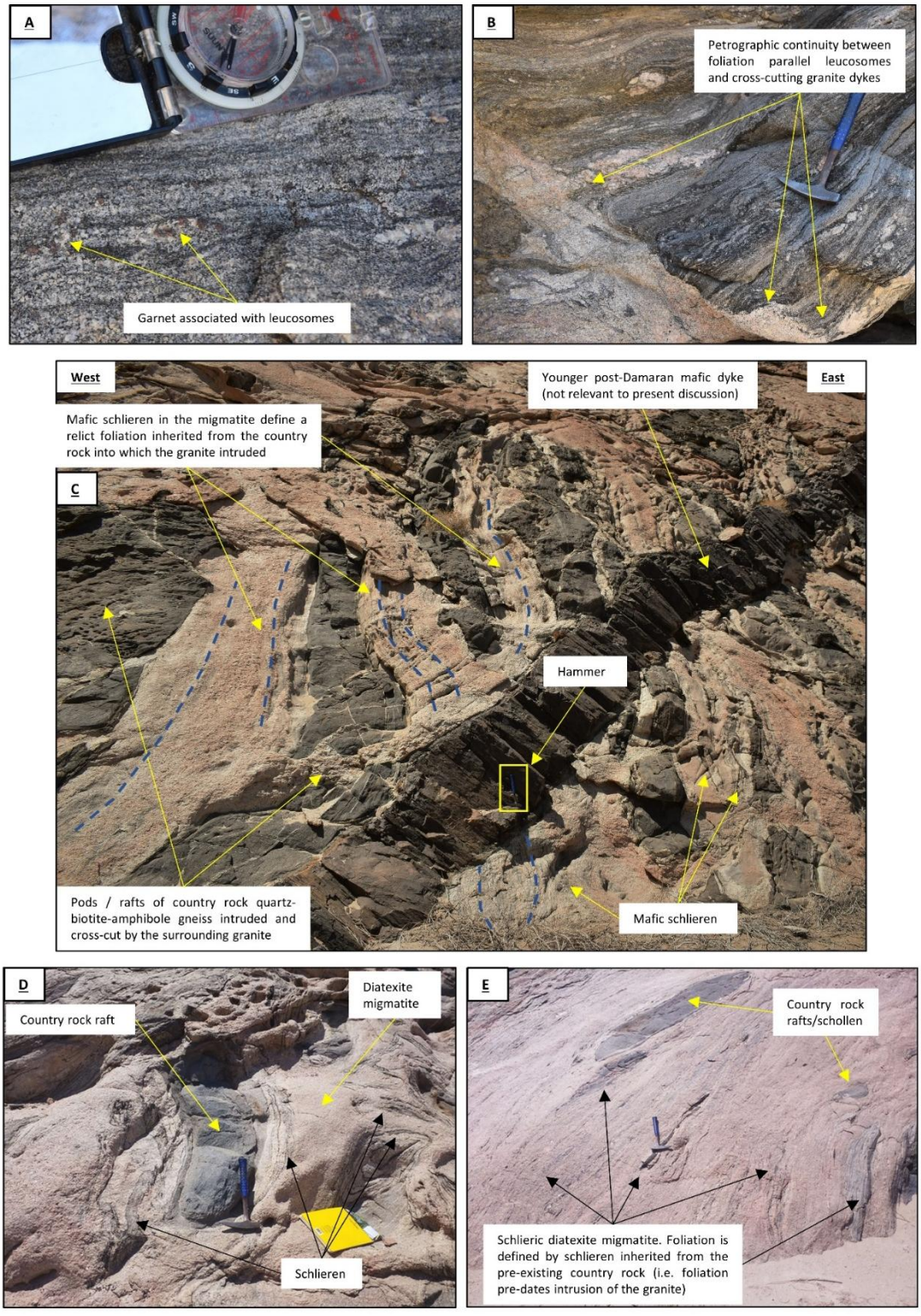

Figure 9 – Migmatites of the Abbabis Complex in the Husabberg Anticlinorium, outcropping west and east of the Husab Gorge. A) Garnet crystals associated with granitic leucosome; B) Foliation-parallel leucosomes show petrographic continuity with larger cross-cutting leucogranite dykes; C, D & E) Schollen and schlieric diatexite migmatites preserving rafts of quartz-biotite-amphibole gneiss.

1

1

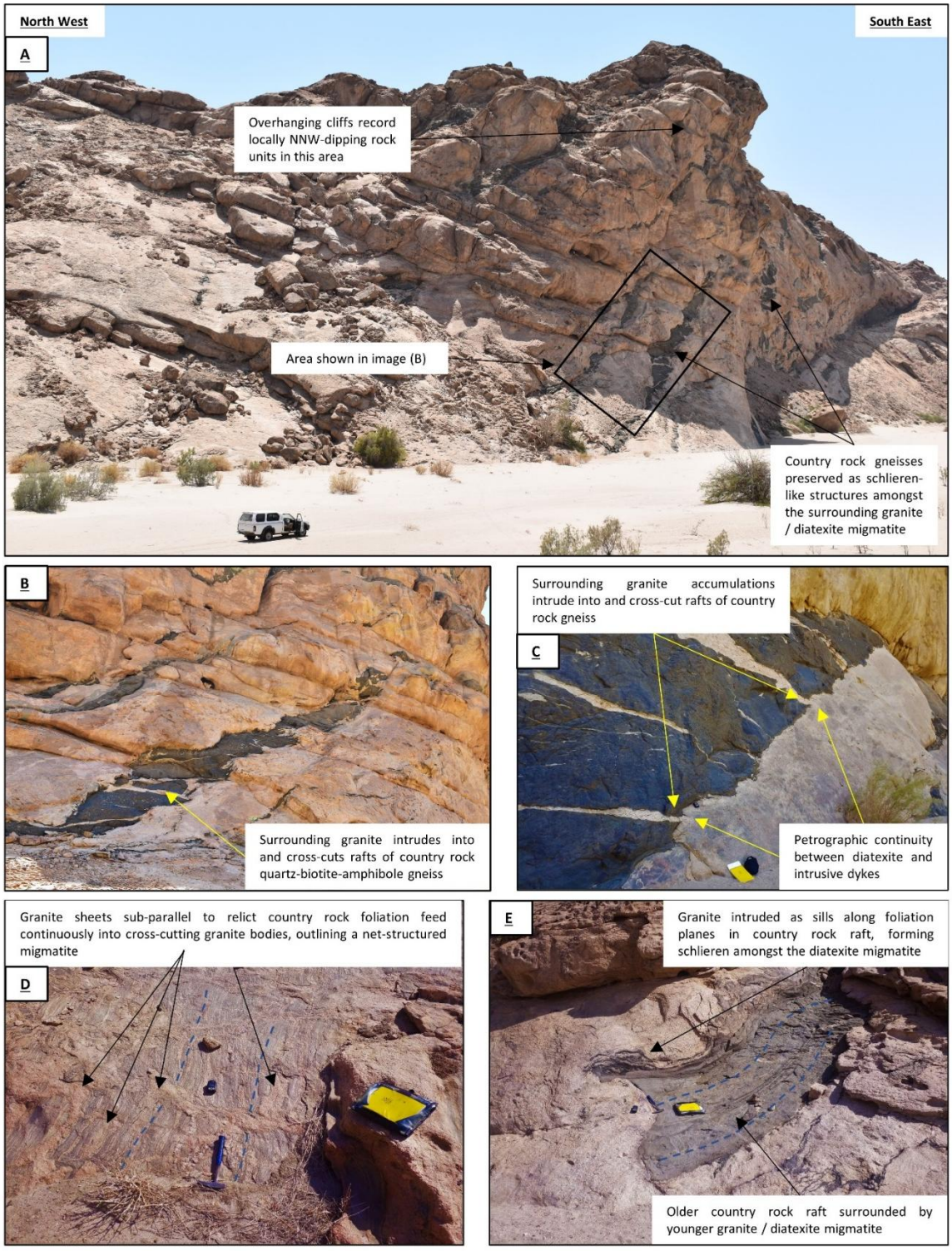

Figure 10 – Diatexite migmatites in the core of the Husabberg Anticlinorium. A) Country rock rafts defining schlieren-like structures amongst granite and migmatite. B & C) Granite intruding into and cross-cutting the country rock rafts. D) A net-structured migmatite. E) Raft of country rock amongst a sea of granite / diatexite migmatite.

2

3.1.2 Larger leucogranite dykes, sills, and plutons

Larger leucogranite dykes, sills and plutons occur amongst the migmatites of the Abbabis Complex.

At the Ida Dome, the proportion of leucogranite increases inwards towards the core of the dome, rising from 40-60 % massive leucogranite amongst the surrounding migmatites on the western limb of the dome, to >80 % massive leucogranite at the deepest structural level in the dome core (Figure 11). The core of the Ida Dome resembles a pluton-like accumulation of leucogranite (Figure 6 & 11). This leucogranite does not contain a pervasively developed solid-state foliation.

At the Husabberg Anticlinorium, another pluton-like accumulation of leucogranite outcrops towards the eastern edge of the dome (Figure 6; Figure 12A). This pluton is several hundred metres thick. It consists of an anastomosing network of leucogranite dykes (Figure 12B), as well as cm-thick leucogranite sills arranged along foliation planes (Figure 12D). Leucogranite dykes and sills merge seamlessly with each other and do not sharply cross-cut one another (Figure 12). Garnet phenocrysts give leucogranites in this area a speckled appearance (Figure 12C).

Figure 11 – Pluton-like accumulation of leucogranite / diatexite migmatite at the deepest exposed level in the core of the Ida Dome.

1

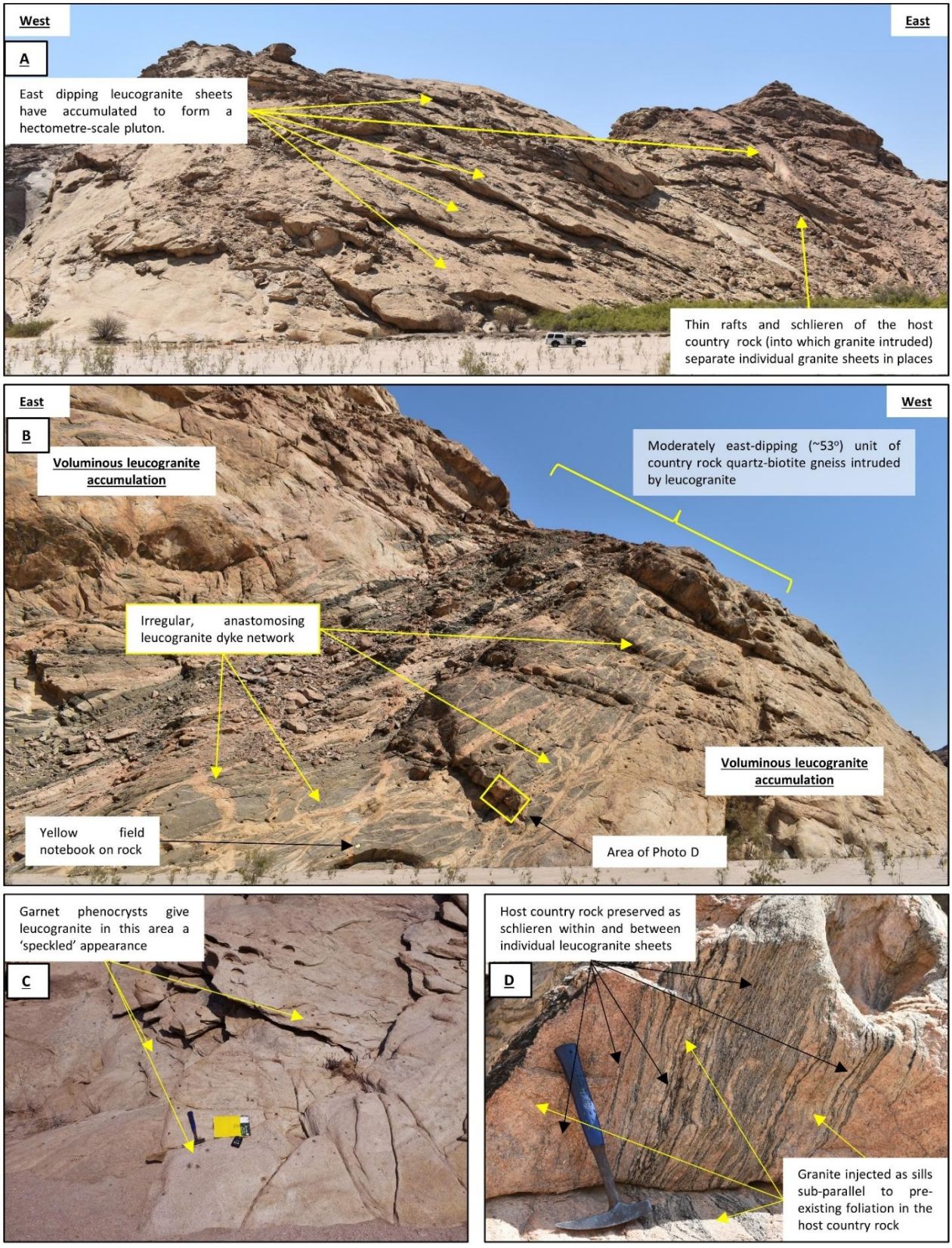

Figure 12 – Pluton-like accumulation of leucogranite near the eastern edge of the Husabberg Anticlinorium. A) Leucogranite pluton formed from the accumulation of individual east-dipping leucogranite sheets. B) Anastomosing leucogranite dykes. C) Garnet phenocrysts. D) Close-up of (B) showing the intrusion of numerous small leucogranite sills oriented sub-parallel to the foliation planes, giving the rock an overall lit-par-lit appearance.

3.1.3 Rafts, schlieren and laterally continuous metasedimentary horizons

Older metamorphic country rocks are preserved as rafts, schlieren, and rarer laterally continuous horizons throughout the cores of the Ida Dome and Husabberg Anticlinorium.

In the Ida Dome, older country rock rafts consist of abundant quartz-biotite+/-amphibole gneisses, as well as some more massive quartzite units up to 20-30 m thick. The quartzites contain heavy mineral laminae of magnetite and ilmenite which locally resemble cross-bedding. Rafts of quartz-clinopyroxene-amphibole+/-garnet gneisses outcrop amongst the diatexite migmatites on the eastern edge of the dome core. Country rock rafts are cross-cut and intruded by the surrounding leucogranite.

At the Arcadia Inlier, country rocks are preserved as elongate pods and rafts of quartz-amphibole-biotite gneiss within the stromatic migmatites. These pods and rafts are concordant with the fabric in the surrounding migmatites (Figure 8A), as well as with the amphibole-biotite schist that outcrops at the base of the Damara Supergroup in the nearby Arcadia Synform (Figure 8D).

In the core of the Husabberg Anticlinorium, an up to 100 m thick carbonate-bearing sequence outcrops along the Swakop River. Mottled diopside-garnet-epidote-gneiss occurs in association with a 10-14 m thick package of marbles and schists. Hyperspectral data (Figure 4) traces this carbonate-bearing sequence for kilometres along strike, where it forms a folded rim around a more massive quartzite unit in the core of the anticlinorium (Figure 5; as also mapped by Barnes, 1981). Additional marble horizons are visible at several locations on hyperspectral imagery in Figure 4. Carbonate sequences also outcrop in the cliff sections west of the Husab Gorge (Figure 4 & 5).

A massive quartzite unit is recognised in the very core of the Husabberg Anticlinorium (Figure 5). Quartz grains (~1 mm size) comprise >60-80% of the rock, with heavy mineral banding (magnetite and ilmenite) arranged in indistinct schlieren-like structures which define a relict fabric. This rock unit is migmatitic, consisting of deformed and rotated migmatitic rafts as well as cross-cutting leucogranites and pegmatites. This quartzite is distinctive on airborne radiometric data due to its low radioactivity relative to the surrounding granites and migmatites (Figure 3).

Elsewhere in the Husabberg Anticlinorium, quartz-biotite+/-amphibole gneiss outcrops as rafts and schlieren within dominantly diatexite migmatite (Figures 9C-9E, 10 & 11). The sheer volume of granite makes it impossible to recognise a clear stratigraphic succession for this gneiss. These rafts and schlieren outcrop throughout a vast area of the Husabberg Anticlinorium (Figure 9 and 10).

3.2 Field geology: Overlying Damara Metasedimentary Supergroup

At the Ida Dome, Neoproterozoic metasedimentary units of the Damara Supergroup overlie the Abbabis Complex in the core of the dome (Figure 5). These units comprise of (1) quartzites and meta-sandstones (*Etusis Formation* of previous studies); (2) an overlying, well-developed, several hundred metres thick sequence of quartz-diopside-epidote-amphibole-biotite gneiss (*Khan Formation* of previous studies; Figure 13), and (3) marble units (*Rössing Formation* of previous studies).

The Arcadia Synform exposes metasedimentary units of the Damara Supergroup near the western edge of the Husabberg Anticlinorium (Figure 5). These units are attributed to the "*Khan*" and "*Rössing*" formations (Barnes, 1981; Longridge, 2012; Kruger and Kisters, 2016). Hyperspectral imagery confirms the existence of distinctive marble units ~1 km north of the Swakop River (Figure 4). The *Khan Formation* is in direct contact with the underlying migmatites of the Abbabis Complex at this area (Figure 8D); the basal *Etusis Formation* is not present.

On the eastern limb of the Husabberg Anticlinorium (Husabberg-Witpoortberg range), the Damara metasedimentary Supergroup outcrops in the core of a tight synform (Figures 5 and 6). Here, it consists of a quartz-biotite gneiss unit immediately overlying the Abbabis Complex; this in turn is overlain by a ~100 metre thick feldspathic quartzite (most similar to the *Etusis Formation* of previous studies). The *Khan*, *Rössing* and *Chuos* formations of the widely accepted Damara Supergroup succession are not present, and thick marble units most closely resembling the *Karibib Formation* of previous studies outcrops in direct contact with quartzites of the *Etusis Formation*. Pelitic gneisses and schists resembling the *Kuiseb Formation* of previous studies cap the sequence in the core of the synform.

Figure 13 – Photomontage (looking towards the south) showing a several-hundred-metre-thick sequence of quartz-diopside-epidote-hornblende-biotite gneiss (i.e., "Khan Formation") of the overlying Damara Supergroup outcropping in a synformal structure above the underlying Abbabis Complex on the western limb of the Ida Dome. Granite intrusion into these overlying metasedimentary units is restricted to a minor volume of leucogranite dykes.

3.3 Field geology: Contact between the Abbabis Complex and Damara Supergroup

At the Ida Dome, the contact between the Abbabis Complex and overlying Damara Metasedimentary Supergroup is difficult to pinpoint. The proportion of intrusive granite increases gradually inwards towards the core of the dome (Figure 14A, 14B & 14C). At the point where granites and migmatites become volumetrically dominant, and a coherent metasedimentary sequence can no longer be recognised (e.g., Figure 11), rocks appear as 'Abbabis Complex' on existing geological maps (Jacob et al., 1978; Geological Survey of Namibia Map Sheet 2214; Longridge et al., 2011; Kruger and Kisters, 2016). However, granites and migmatites of the Abbabis Complex universally intrude into and cross-cut the overlying Damara Supergroup (Figure 14A-C). The overlying metasedimentary units do not cross-cut the underlying granites or migmatites.

At the Arcadia Synform, the contact with migmatites of the underlying Abbabis Complex is slightly overturned on the western limb of the synform (Figure 8D). This contact is exposed as a jagged and irregular, yet relatively sharp transition occurring over just a few metres, from migmatites of the Abbabis Complex into amphibole-rich schists of the *Khan Formation*. The foliation in the *Khan Formation* is concordant with the fabric in the underlying migmatites; an angular unconformity is not observed (Figure 8D). Leucogranite dykes, which show petrographic continuity with leucosomes in the underlying migmatites (Figure 8C), intrude across the contact and cut through the overlying Damara metasedimentary Supergroup (Figure 8D – note that this contact is slightly overturned).

On the eastern limb of the Husabberg Anticlinorium, the contact cannot be sharply defined at any single location. The proportion of leucogranite and migmatite increases inwards towards the core of the dome. Eventually, the granites and migmatites become so voluminous that a metasedimentary succession can no longer be clearly recognised (Figure 15); at this point rocks appear as part of the Abbabis Complex on existing maps (Jacob et al., 1978; Geological Survey of Namibia Map Sheet 2214). However, metasedimentary units do not cross-cut the underlying granites and migmatites of the Abbabis Complex. In contrast, granites and migmatites intrude into and cross-cut the overlying metasedimentary units.

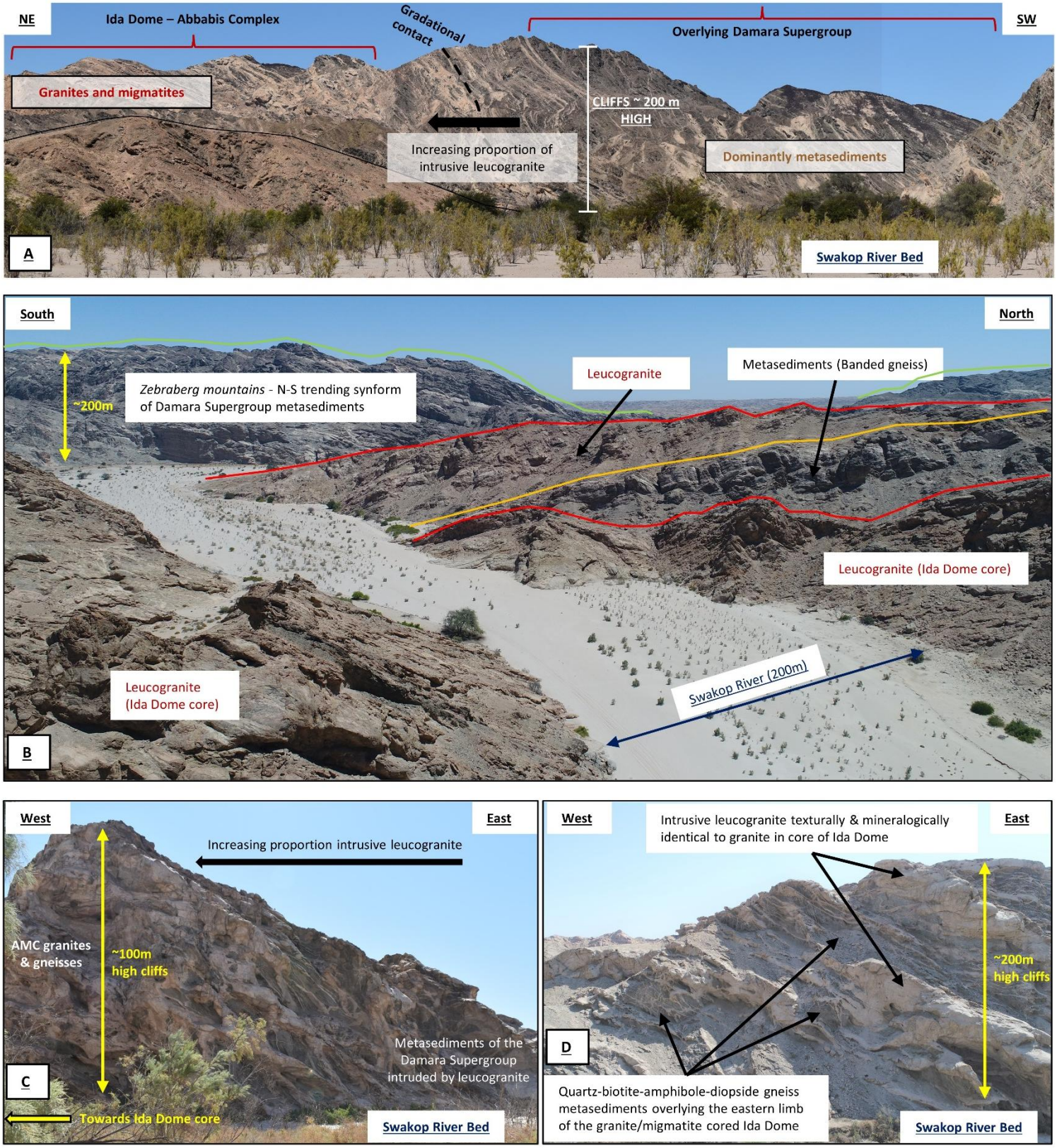
NE
Ida Dome – Abbabis Complex
Gradational contact
Overlying Damara Supergroup
SW
Granites and migmatites
CLIFFS ~ 200 m HIGH
Increasing proportion of intrusive leucogranite
Dominantly metasediments
A
Swakop River Bed
South
North
~200m
Zebraberg mountains - N-S trending synform of Damara Supergroup metasediments
Leucogranite
Metasediments (Banded gneiss)
Leucogranite (Ida Dome core)
Swakop River (200m)
Leucogranite (Ida Dome core)
B
West
East
Increasing proportion intrusive leucogranite
AMC granites & gneisses
~100m high cliffs
Metasediments of the Damara Supergroup intruded by leucogranite
C
Towards Ida Dome core
Swakop River Bed
West
Intrusive leucogranite texturally & mineralogically identical to granite in core of Ida Dome
East
~200m high cliffs
D
Quartz-biotite-amphibole-diopside gneiss metasediments overlying the eastern limb of the granite/migmatite cored Ida Dome
Swakop River Bed

1

2

3

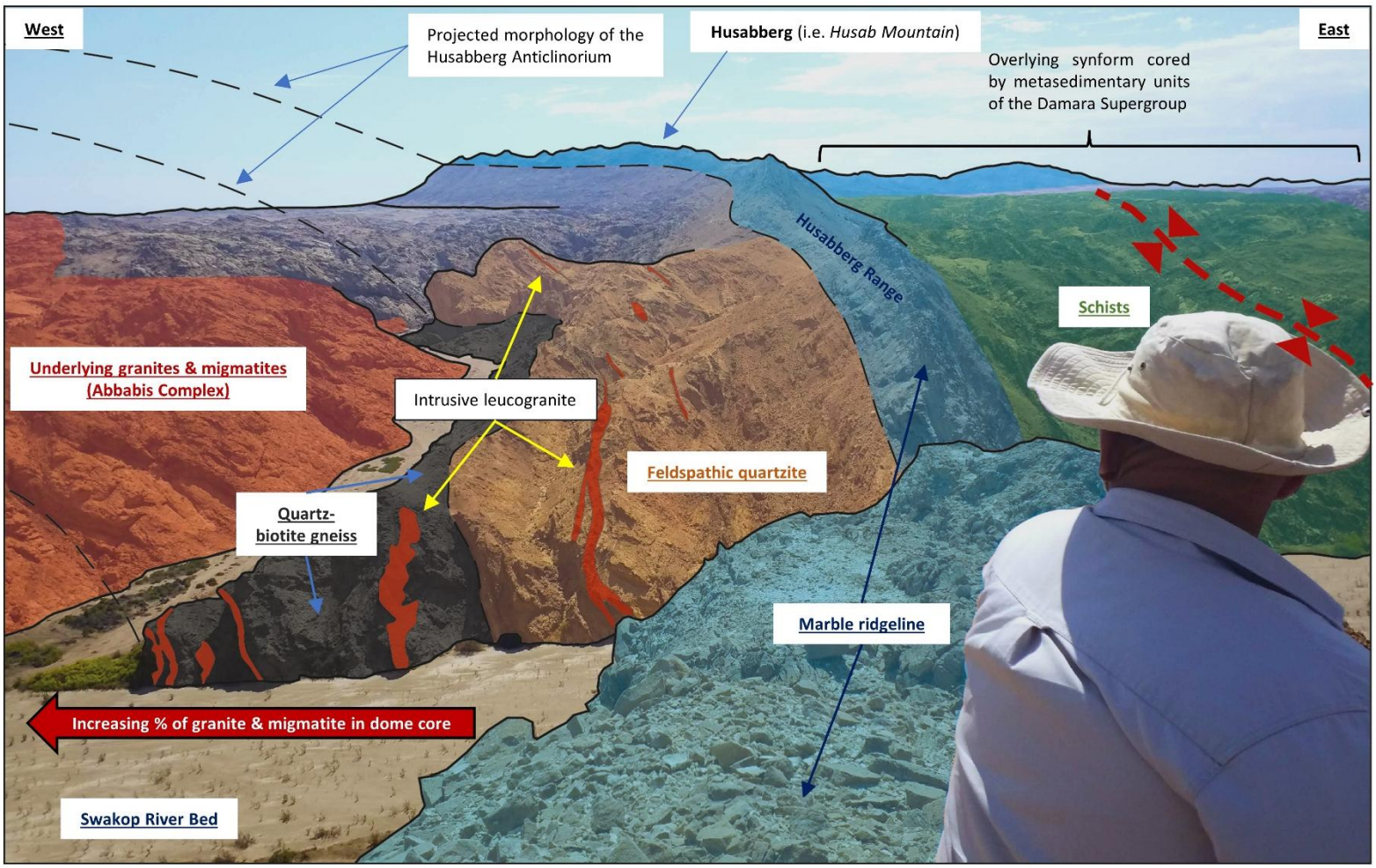

Figure 15 – View towards the north, highlighting how granites and migmatites of the Abbabis Complex intrude into and cross-cut the overlying metasedimentary units of the Damara Supergroup on the eastern limb of the Husabberg Anticlinorium

Figure 14 (previous page)- Contact between granites and migmatites of the Abbabis Complex in the core of the Ida Dome with the overlying metasedimentary units of the Damara Supergroup. A) Panoramic photomontage showing the contact on the western limb of the dome. B) Aerial photograph looking outwards from the core of the Ida Dome, showing how leucogranites and migmatites in the dome core are overlain by Damara Supergroup metasediments on the dome limb. C) Photo from the Swakop River showing a gradational contact on the eastern limb of the Ida Dome. D) Metasedimentary units of the Damara Supergroup outcropping in a cliff section on the eastern limb of the Ida Dome. The metasediments are heavily intruded by a leucogranite dyke network.

3.4 Field geology: Relationship of leucogranites in the Abbabis Complex to leucogranites intruding into the overlying Damara Supergroup

Leucogranite accumulations comprise up to 80% of the Abbabis Complex in the core of the Ida Dome (Figure 11). Similar leucogranites intrude into the overlying *Khan Formation* of the Damara Supergroup as a voluminous dyke network (Figure 14D). A clear age relationship cannot be distinguished on the basis of cross-cutting relations; the leucogranites appear to form an interconnected, anastomosing, network where individual leucogranite-bearing structures merge seamlessly with one another (Figure 11 and 14). Leucogranites in both locations are white-cream-pink in colour, dominantly composed of quartz and feldspar, and are typically fine-grained (1-2 mm) with more pegmatitic patches (crystals 3-7 cm in size).

3.5 Geochronological data for the Nosib Group of the Damara Supergroup and the Abbabis Complex

Available geochronological data for the Abbabis Complex and lower Nosib Group (Khan and Etusis formations) of the Damara Supergroup is compiled in Figure 16. Both populations show two prominent age peaks at c. 1 Ga and c. 2 Ga. The Nosib Group exhibits a particularly strong c. 1 Ga population with a subordinate c. 2 Ga component. The overall age spectra of both populations overlaps substantially.

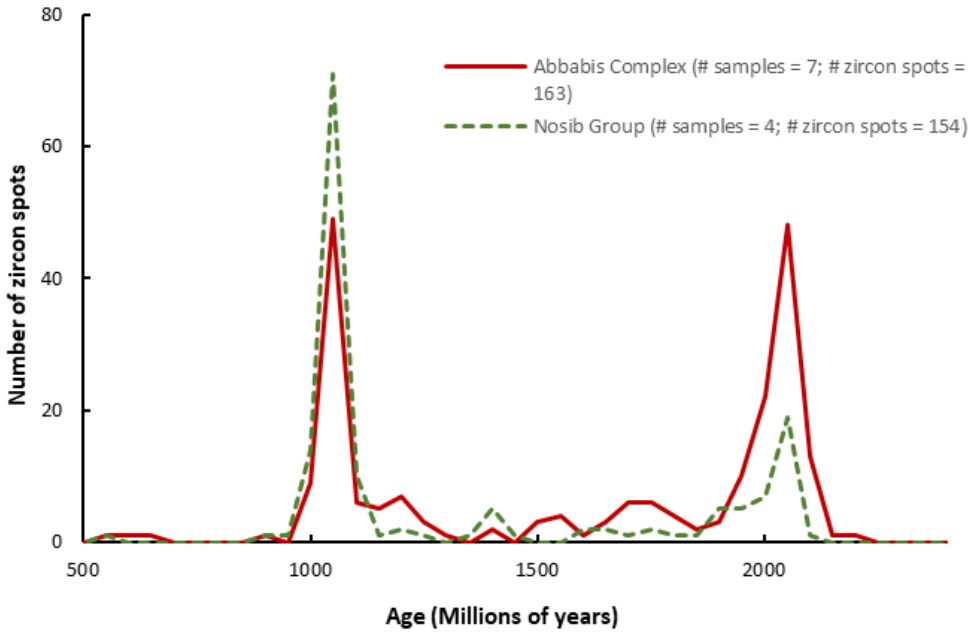

Figure 16 – Compilation of existing U-Pb zircon age data for the Abbabis Complex and the Nosib Group (Khan & Etusis Formations) of the Damara Supergroup. Data sources: Kroner et al., 1991; Foster et al., 2015; Longridge et al., 2018; Goslin, 2019.

3.6 Geochemical Data

The geochemical dataset encompasses:

- ***Leucogranite dykes***: 12 samples of leucogranite dykes intruding into the Khan Formation of the Damara Supergroup on the western, eastern, and southern limbs of the Ida Dome.
- ***Leucosomes from Abbabis Complex migmatites***: 8 samples of leucosomes from migmatites in the Abbabis Complex in the core of the Ida Dome.

3.6.1 Major element behaviour

Leucogranite dykes and leucosomes have similar major element compositions. Both populations have high silica contents; dykes average 74.22% while leucosomes average 74.63% (Figure 17). Leucosomes are slightly more Ca-rich, Fe2O3(t)-rich, and TiO2-rich, while dykes are slightly more K2O-rich (Figure 17). All samples bar one are weakly peraluminous; dykes have a mean Alumina Saturation Index of 1.02 (range = 0.95 - 1.07) while leucosomes sit at 1.03 (range = 1.02 - 1.05) (Figure 18). One leucogranite dyke was metaluminous (ASI = 0.95).

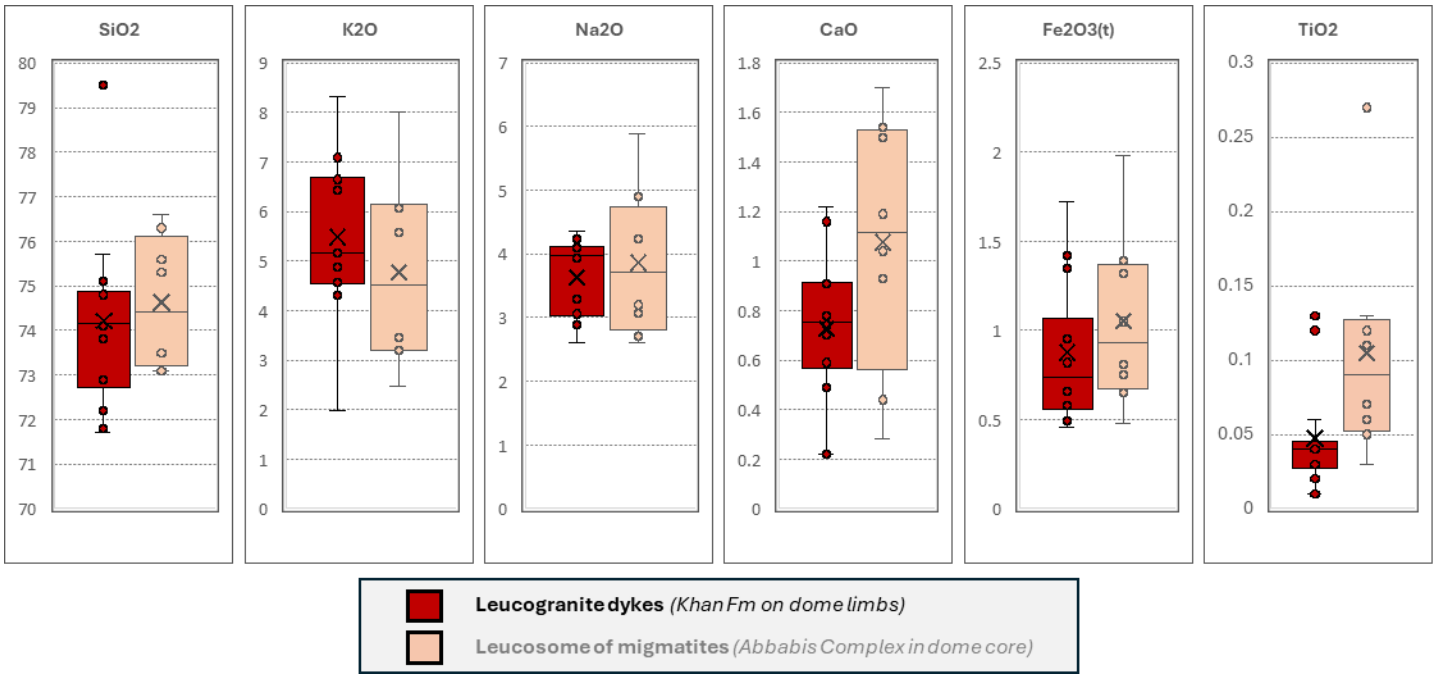

Figure 17 - Box and whisker plots of major element oxides by weight % in leucogranite dykes vs leucosomes.

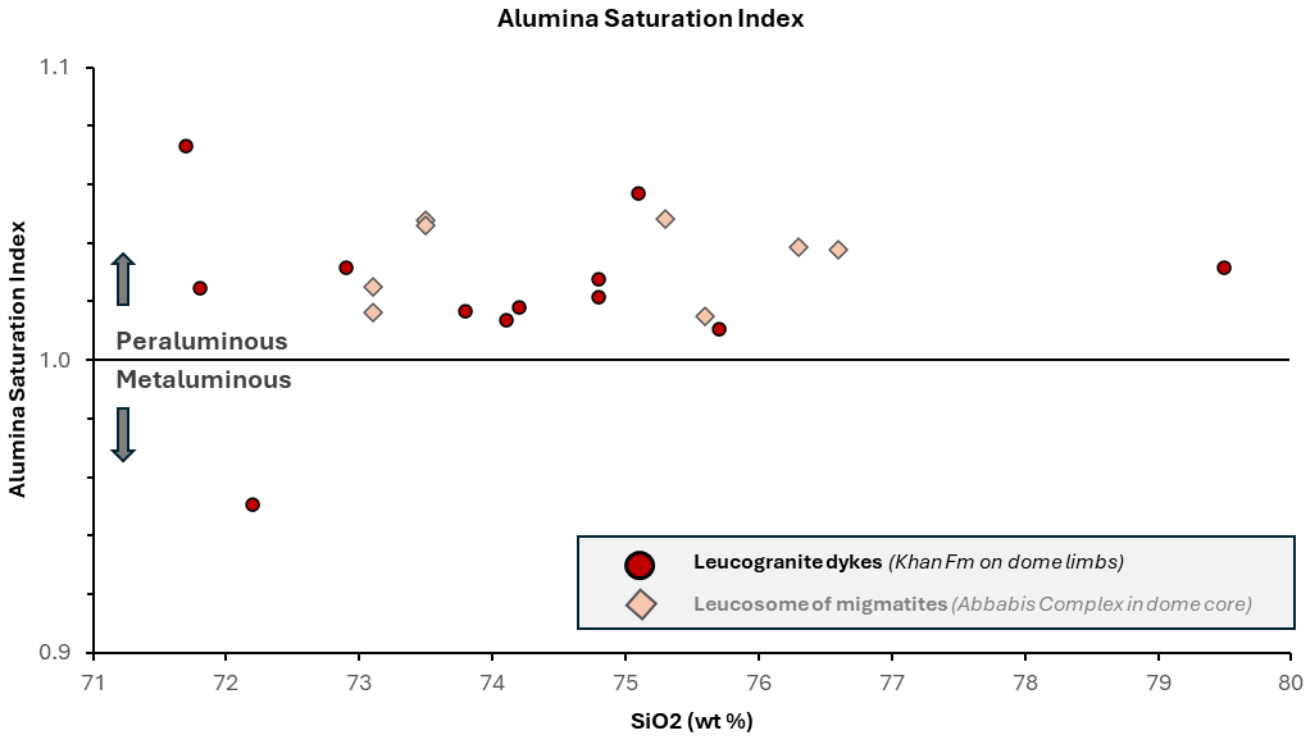

Figure 18 - Alumina saturation index (molar Al/(Ca+Na+K) plotted against silica

3.6.2 Trace element behaviour - Large-ion Lithophile Elements (LILE) & High Field Strength Elements (HFSE)

Leucogranites and leucosomes have similar overall trends in trace element composition (Figure 19). They are depleted in Cr and Co and notably enriched in Rb, Ba, Th, and U.

While the trend is similar, there are differences in individual trace element concentrations. Abbabis Complex leucosomes are more enriched in Sr, Y, Zr, Hf, Ba and Th. Meanwhile, leucogranite dykes are more enriched in Ta, W, and U, and marginally more enriched in Rb, Nb, and Cs (Figure 19).

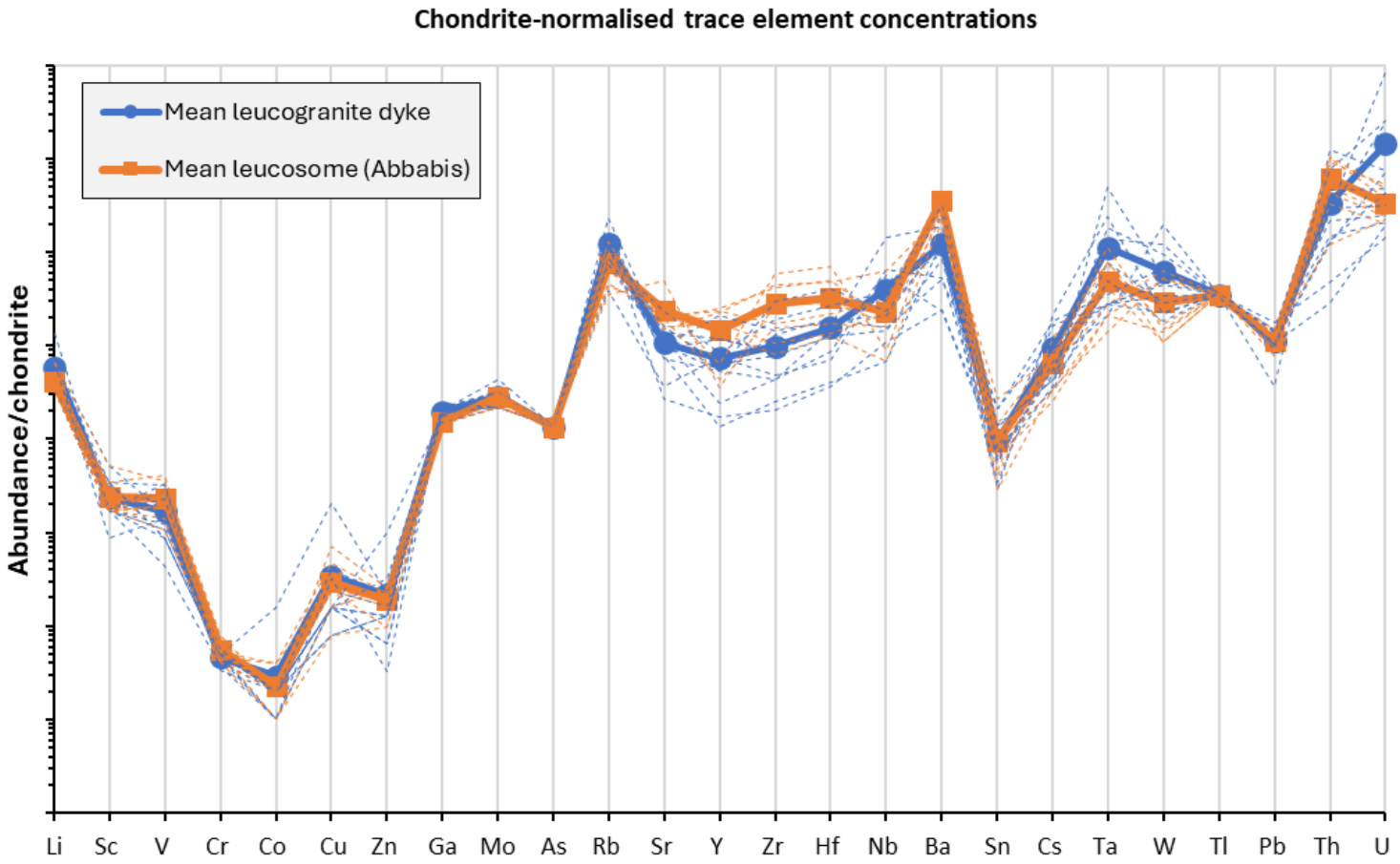

Figure 19 - Chondrite-normalised trace element concentrations. Chondrite values from Anders and Grevesse (1989).

3.6.3 Rare Earth Element (REE) behaviour

Leucogranites and leucosomes show very similar trends in REE behaviour (Figure 20). They are light REE enriched and have a steep negative slope from La to Sm, followed by a flatter profile from Gd to Lu. Both populations have a clear negative Eu anomaly, although this is slightly larger in the dykes than the leucosomes. However, leucogranite dykes are significantly depleted in total REE abundance relative to the leucosomes (Figure 20).

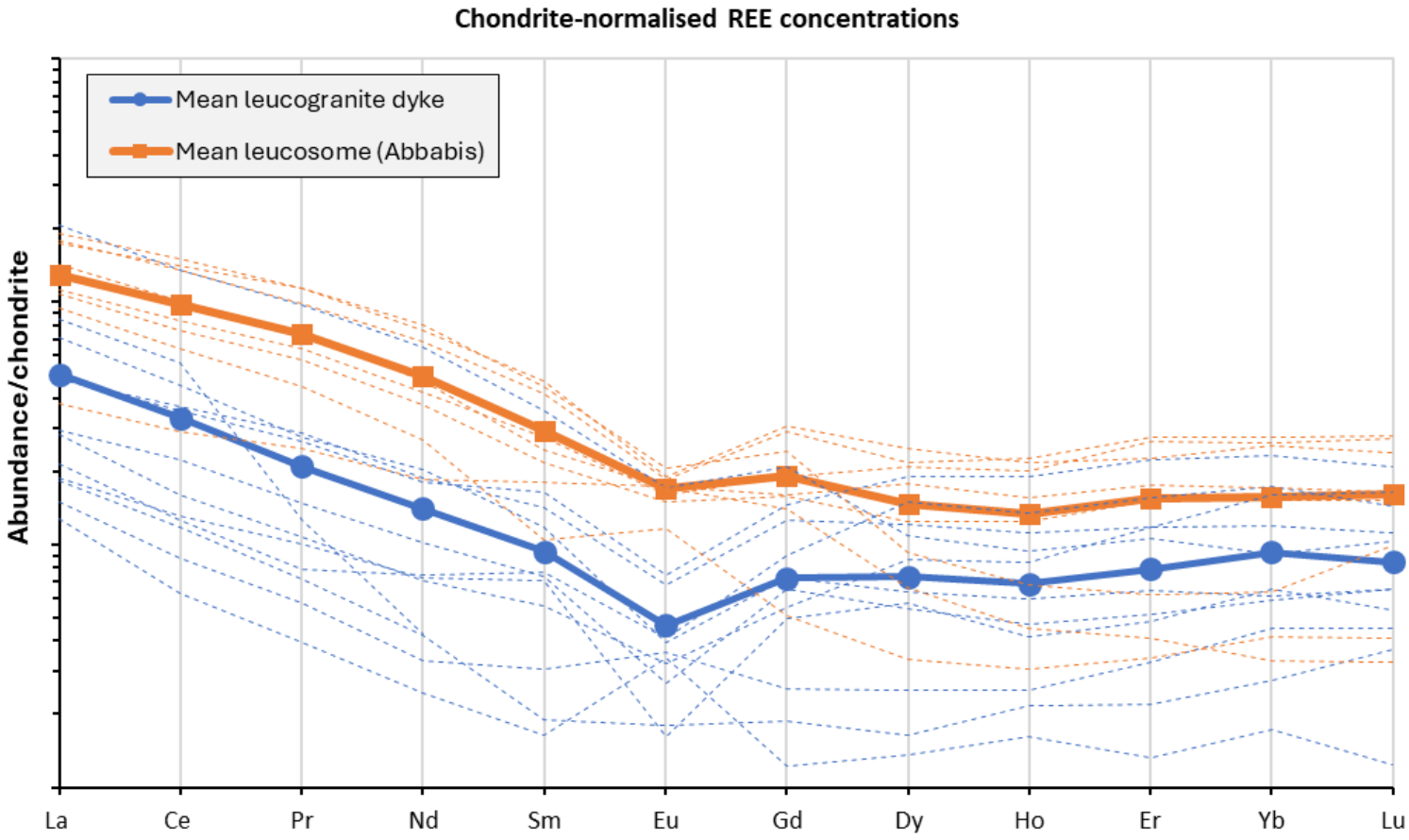

Figure 20 - Chondrite-normalised rare earth element (REE) concentrations. Chondrite values from Anders and Grevesse (1989).

3.6.4 Element pair and ratio plots

Specific elements are removed from the melt as minerals crystallise, meaning melt composition evolves along predictable trends. Element pair and ratio plots help to isolate specific mineral control, test closed system fractional crystallisation, and separate fractionation from melting or mixing processes (see Appendix I). Results for dyke and leucosome samples are plotted in Figure 21:

A. ***Ba vs Sr***: Strong positive correlation - dykes have lower Ba and Sr concentrations than the leucosomes.
B. ***Rb/Sr vs Sr***: Strong inverse trend - dykes extend to lower Sr and higher Rb/Sr values than the leucosomes.
C. ***Eu/Eu* vs Sr***: Moderate positive correlation - leucosomes generally have higher Sr concentrations and higher Eu/Eu* ratios than most dykes. However, two dykes are outliers with comparatively high Eu/Eu* ratios at low Sr concentrations.
D. ***K/Rb vs Rb***: Strong inverse trend - dykes have higher Rb concentrations and lower K/Rb ratios than the leucosomes.
E. ***Th vs La***: Strong positive correlation – leucosomes and dykes are clustered along a positive trend. Dykes show slightly more scatter than leucosomes and plot at slightly lower La concentrations at given Th concentration. Dykes have lower Th and La concentrations than leucosomes overall.
F. ***Zr vs Hf***: Strong positive linear trend with tight clustering along trend and no deviation. Leucosomes extend to higher Zr and Hf concentrations overall, with dykes dropping to lower concentrations. There is overlap between both populations.
G. ***Th vs Zr***: Dykes and leucosomes show positive correlation along the same trend. Dykes generally plot at lower Th and Zr concentrations than the leucosomes.
H. ***Zr vs Y***: Broad positive correlation overall. Leucosomes occupy higher Zr and Y than dykes, with both populations lying laong the same trend.
I. ***Ta vs Nb***: Strong positive correlation. Leucosomes and dykes are tightly clustered along the same slope. Both populations overlap, but dykes extend to slightly higher Ta and Nb values while leucosomes drop to slightly lower concentrations.
J. ***Nb/Ta vs Nb***: No correlation - the Nb/Ta ratio remains constant at different Nb concentrations.
K. ***Y vs Yb***: Strong positive correlation. All samples plot along a tight linear trend. Both populations overlap, but leucosomes extend to higher Y and Yb concentrations overall while dykes drop to lower absolute values.

1

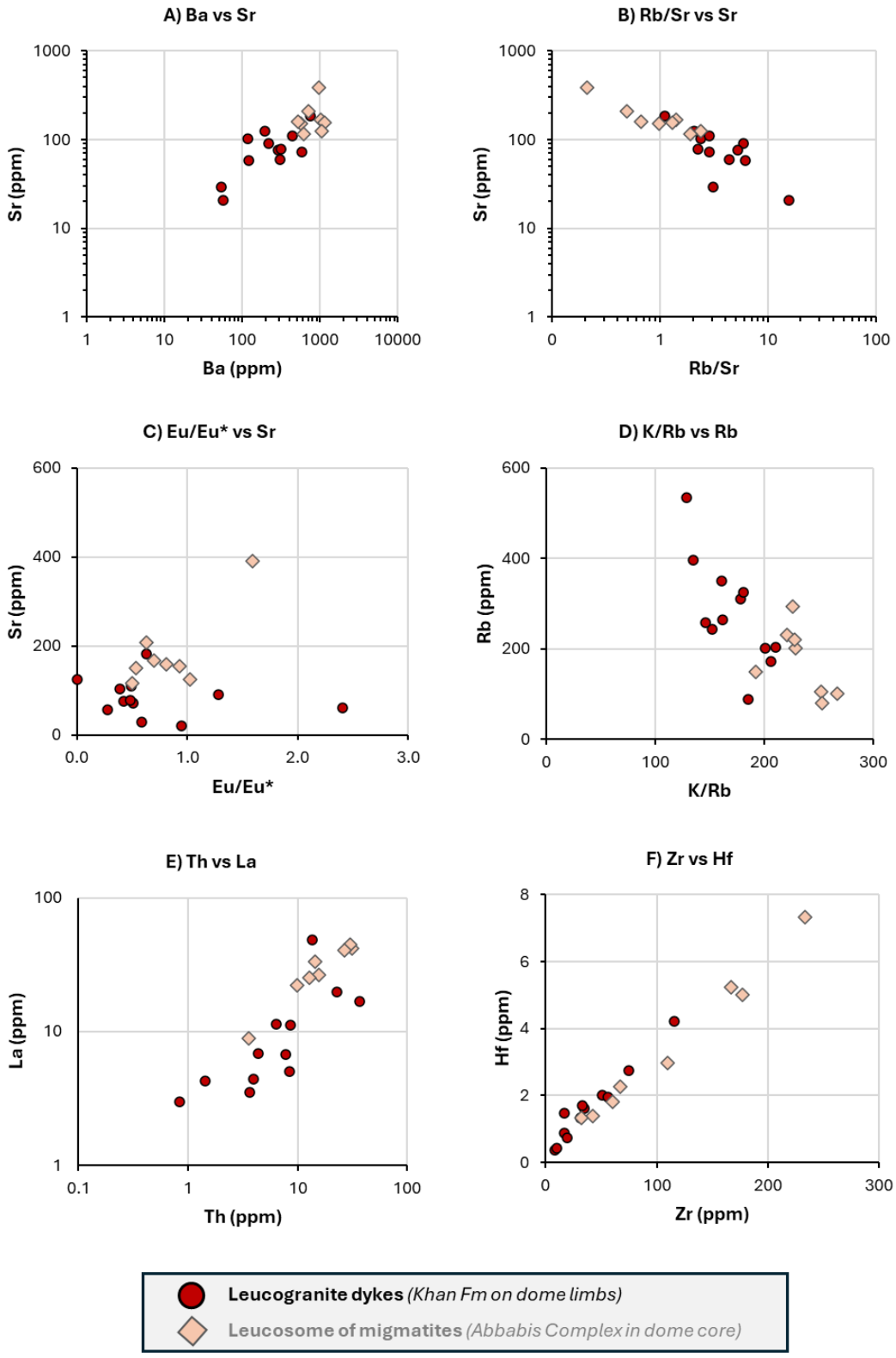
A) Ba vs Sr
Sr (ppm)
Ba (ppm)
B) Rb/Sr vs Sr
Sr (ppm)
Rb/Sr
C) Eu/Eu* vs Sr
Sr (ppm)
Eu/Eu*
D) K/Rb vs Rb
Rb (ppm)
K/Rb
E) Th vs La
La (ppm)
Th (ppm)
F) Zr vs Hf
Hf (ppm)
Zr (ppm)
Leucogranite dykes (Khan Fm on dome limbs)
Leucosome of migmatites (Abbabis Complex in dome core)

2

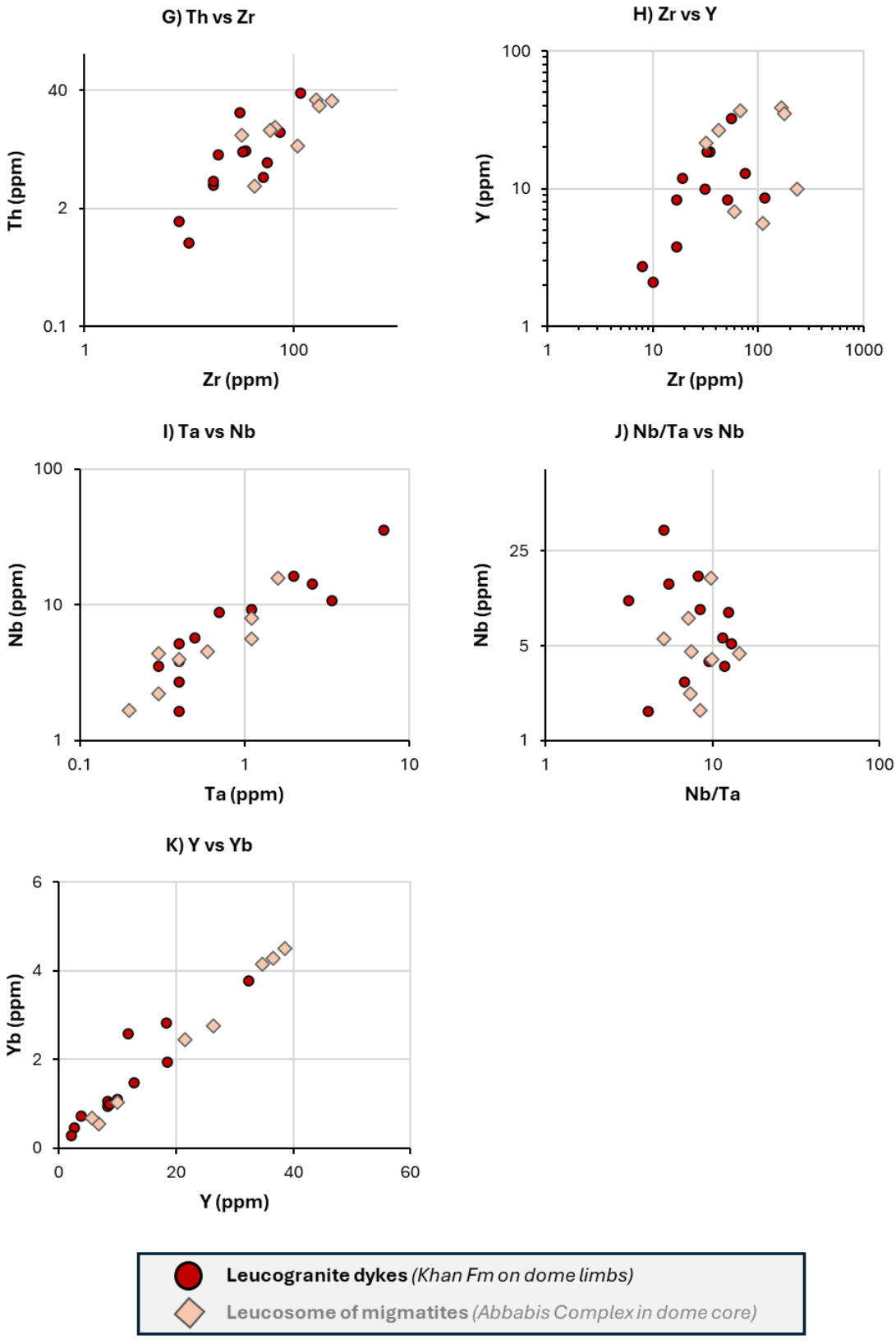

Figure 21 - Element pair and ratio plots for leucogranite dykes and leucosomes of migmatites. A) Ba vs Sr, B) Rb/Sr vs Sr, C) Eu/Eu vs Sr, D) K/Rb vs Rb, E) Th vs La, F) Zr vs Hf, G) Th vs Zr, H) Zr vs Y, I) Ta vs Nb, J) Nb/Ta vs Nb, K) Y vs Yb*

4. INTERPRETATION & DISCUSSION

4.1 Field constraints on the nature of the Abbabis Complex in the Ida Dome and Husabberg Anticlinorium

The Abbabis Complex in the core of the Ida Dome and Husabberg Anticlinorium shows all features consistent with a mid-crustal migmatite-granite complex. It consists of (1) metatexite and diatexite migmatites (Figure 7 to 10), (2) larger leucogranite dykes, sills and pluton-like accumulations (Figure 11 and 12), and (3) older country rocks preserved as rafts and schlieren.

The contact between the Abbabis Complex and overlying Damara Supergroup is poorly defined on the limbs of both domes. There is no field evidence demarcating an angular unconformity or distinct depositional horizon. Instead, the contact appears to be an intrusive contact, where underlying granites consistently intrude into and cross-cut the overlying metasedimentary units of the Damara Supergroup (Figure 14 & 15). Units mapped as 'Abbabis Complex' on existing maps correspond to domains where granite and migmatite is volumetrically dominant and a coherent metasedimentary succession can no longer be recognised (Figure 5 & 6). However, metasedimentary units do continue to outcrop as isolated rafts, schlieren and occasional laterally continuous horizons amongst the intrusive migmatites in the cores of both domes.

No systematic cross-cutting relationship distinguishes leucogranite within the Abbabis Complex from leucogranite dykes intruding into the overlying Damara Supergroup. These dykes appear to form an interconnected melt-bearing network which transcends across the mapped boundary (Figure 8D, 14 & 15). This is consistent with these dykes facilitating melt transfer out of the migmatite complex and upwards into overlying levels of the crust.

4.2 Geochemical constraints on migmatite-dyke connectivity

Whole-rock geochemical data provides an independent check on the hypothesis that migmatites and leucogranite dykes were part of an interconnected melt transfer network in the mid-crust of the Damara Orogen. Eight samples of granitic leucosome from migmatites of the Abbabis Complex in the core of the Ida Dome have been compared to 12 samples of leucogranite dykes intruding into the overlying Damara Metasedimentary Supergroup on the dome limbs.

The weakly peraluminous nature of 19 of the 20 samples (Figure 18) implies that these are S-type crustal melts derived from metasedimentary protoliths. Similar major element compositions (Figure 17), along with near-parallel patterns on trace element spider diagrams (Figure 19) and similar behaviour on REE spider diagrams (Figure 20), argues for a close genetic relationship between the dykes and leucosomes – consistent with derivation from a common magmatic system. Dykes and leucosomes fall along near identical trends on element pair and ratio plots (Figure 21), indicating that similar mineralogical controls and differentiation trends governed both populations.

Geochemical data shows that the dykes are consistently more evolved than the leucosomes. Dykes have slightly higher K2O contents - consistent with k-feldspar enrichment. Dykes have slightly lower CaO and TiO2 contents relative to the leucosomes (implying plagioclase and biotite/ilmenite/titanite removal, respectively) (Figure 17). More significantly, the dykes have a relatively stronger Eu anomaly (Figure 20), implying more plagioclase fractionation. This is consistent with lower Sr and higher Rb/Sr ratios in the dyke population (Figure 21B), since Rb stays incompatible while Sr is removed in plagioclase. Dykes fall lower than leucosomes on the Ba vs Sr plot (Figure 21A), consistent with greater plagioclase and K-feldspar removal. Dykes have higher Rb concentrations and lower K/Rb ratios than leucosomes (Figure 21D), again consistent with them being more evolved, since Rb is more incompatible than K and hence concentrates in late melt. Dykes and leucosomes each extend towards opposite ends of element pair and ratio plots, while also consistently overlapping in the middle (Figure 21); this is consistent with differentiation of a single magmatic system, in which the dykes represent relatively more evolved and pure melt than the leucosomes.

In summary, whole rock geochemical data is consistent with an interpretation that leucogranite dykes in the overlying Damara Supergroup are part of the same magmatic system as migmatites in the underlying Abbabis Complex. The more evolved signature of the dykes relative to the leucosomes is consistent with their distal location on the overlying limbs of the dome. This supports field observations in suggesting that the dykes facilitated the extraction and upward ascent of leucocratic melt out of the migmatite complex and into the overlying metasedimentary units of the Damara Supergroup.

4.3 Comparison of field data to the prevailing c. 1 or 2 Ga pre-Damaran basement model

The prevailing interpretation of the Abbabis Complex as an unconformably older c. 1 or 2 Ga basement terrain throughout the southern Central Zone (Smith, 1965; Marlow, 1981; Barnes, 1981; Jacob et al., 1983; Brandt, 1987; Lehtonen et al., 1996; Longridge, 2012) is based on the complexity of rock

textures and fabrics in the Abbabis Complex, the different lithology of the Abbabis Complex (dominantly granitic gneiss) vs the overlying Damara Metasedimentary Supergroup, and local interpretations that a basal conglomerate in the Etusis Formation contains clasts resembling granitic rocks of the Abbabis Complex. The absence of an angular unconformity at the contact with the overlying Damara Supergroup has previously been attributed to overprinting by younger deformation and tectonism during the Damara Orogeny (Oliver, 1994, 1995).

However, in this study we found that:

i. The complexity of rock textures and fabrics in the Abbabis Complex is due to migmatitic features; these record mesoscale pervasive melt migration along foliation planes and through cross-cutting shear bands (Figure 7 to 9). Despite the complexity of migmatite fabrics and textures, the Abbabis Complex in the core of the Ida Dome and Husabberg Antilincorium preserves a similar strain record to the overlying Damara Metasedimentary Supergroup; fold axes plunge shallowly NE-SW, axial planes dip variably due to constrictional strains, and reverse shear on both SE- and NW-dipping dome limbs can be attributed to bulk coaxial NW-SE shortening during Congo-Kalahari collision (Jones, 2026 - *manuscript in review*). While some studies locally report an older pre-Damaran fabric in the Abbabis Complex (Longridge, 2012; Kroner, 1984; Kroner et al., 1991), care must be taken as progressive deformation can also form overprinting relations which mimic the appearance of older fabrics (Fossen et al., 2019). An older basement complex cannot be distinguished in our study area on the basis of different strain histories.

ii. Our lithological description of the Abbabis Complex is broadly similar to that described by previous studies - an older metasedimentary suite is cross-cut by a volumetrically more abundant assortment of orthogneisses, granitic gneisses, leucocratic augen gneisses and (in places) intrusive granites (Smith, 1965; Marlow, 1981; Barnes, 1981; Sawyer, 1979; Jacob et al., 1983; Brandt, 1987; Longridge, 2012). However, the granitic component in these rocks consistently cross-cuts the metamorphic fabric throughout the study area (Figure 7 to 12). These textures and cross-cutting relations are consistent with migmatites recording partial melting, melt migration and melt accumulation in the crust; they are not consistent with deformation of an older granite suite.

iii. We have not observed an unconformity, distinct stratigraphic break, or localised shear zone or high strain zone along the contact between the Abbabis Complex and Damara Supergroup (c.f. Oliver, 1994, 1995). A basement-cover shear zone would be expected to transpose dykes towards parallelism with the contact, but this is not observed. In contrast, the contact appears intrusive

and leucogranite dykes locally intrude across the contact at a variety of angles (Figure 8D, 14 & 15).

4.4 Evolution of a syn-orogenic migmatite-granite complex in the Ida Dome and Husabberg Anticlinorium

Here, we outline how rocks and field relations are consistent with a syn-orogenic migmatite-granite complex in the core of the Ida Dome and Husabberg Anticlinorium:

Partial melting, melt migration & melt accumulation: Local evidence for in-situ partial melting is observed within the Abbabis Complex, where coarse garnet phenocrysts are associated with leucosomes in patch migmatites (Figure 9A). This is consistent with melting reactions reported in nearby country rocks (Ward et al., 2008; Jung et al., 2019). The volume of granite present in the core of the Ida Dome and Husabberg Anticlinorium is almost certainly too large for these migmatites to have formed entirely via in-situ partial melting (e.g., Figure 11 & 12). Fabrics and textures are consistent with mesoscale melt migration along foliation planes, through cross-cutting shear bands, and along larger dyke-like structures to form larger granite accumulations (Figures 7 to 12). Pervasive mesoscale melt migration in this way is well documented from orogenic belts worldwide (Weinberg & Searle, 1998; Weinberg, 1999; Brown, 2007, 2013). Migmatites in the Abbabis Complex closely resemble 'injection migmatites' described in other orogenic belts.

The Abbabis Complex – Damara Supergroup contact: When melt solidus temperatures are lower than country rock temperatures, then small volumes of melt can migrate pervasively along foliation planes and through shear bands without freezing (Weinberg, 1999; Leitch & Weinberg, 2002; Brown, 2007; Cruden and Weinberg, 2018). However, this is restricted to higher-temperature conditions in mid- to lower-crustal settings, since colder overlying crustal rocks will cause these small bodies of melt to freeze at the 'magma front'. Further granite intrusion above the magma front is typically restricted to dykes, since dykes can propagate faster and transport larger magma bodies which are better insulated against freezing (Cruden and Weinberg, 2018).

Field relations indicate that the contact between the Abbabis Complex and overlying Damara Supergroup is intrusive (Section 3.3; Figure 14 & 15). Below this contact, melt is pervasively distributed along foliation planes and in small-scale shear bands within migmatites (Figure 7 to 12). Above this contact, granite intrusion is limited mostly to anastomosing dyke networks which cross-cut coherent metasedimentary units of the Damara Supergroup (Figure 14 & 15). The geometry and morphology of

this contact, occurring gradually over distance of tens to hundreds of metres, appears consistent with that of a 'magma front' (Figure 22).

Leitch and Weinberg (2002) demonstrated that the position of a magma front is not fixed in space or time, since pervasive magma intrusion can locally increase the temperature of country rocks via heat advection; this allows the magma front to push higher into overlying rocks. The height of the magma front relative to the country rock stratigraphy may therefore vary spatially from one dome structure to another. This can explain the absence of the *Etusis Formation* at the Arcadia Synform (Figure 8D), and it may also explain why the metasedimentary succession overlying the eastern limb of the Husabberg Anticlirnorium differs from that described for the Damara Supergroup elsewhere in the southern Central Zone (Section 3.2).

Metasedimentary source material for the leucogranites: The weakly peraluminous nature of leucogranites and leucosomes in the Abbabis Complex (Figure 18) implies formation via partial melting of metasedimentary rather than igneous source rocks. Metasedimentary units are preserved as rafts, schlieren, and laterally continuous horizons amongst the Abbabis Complex; these form the older country rock protoliths invaded by many of the migmatites (Section 3.1.3). The metasedimentary protoliths to migmatites in the Abbabis Complex are credible source rocks for peraluminous leucogranites (Figure 22).

Metamorphic conditions: High temperature metamorphic conditions are required to form the migmatite structures in the Abbabis Complex. Regional temperatures reached ~800^{O}C throughout the southwestern Central Zone during the latter stages of the Damara Orogeny (Longridge et al., 2017; Jung et al., 2019; MacRoberts et al., 2025). This high-temperature thermal event was contemporaneous with widespread leucogranite magmatism at c. 520 Ma (Longridge et al., 2017; Jung et al., 2019; MacRoberts et al., 2025). This high-temperature granulite-facies metamorphic event provides ideal metamorphic conditions for the formation of a widespread migmatite-granite complex of the type described here (Figure 22).

4.5 Interpretation of Zircon Ages

Published CL imaging and U–Pb datasets from the Abbabis Complex document a dominant population of oscillatory-zoned, euhedral to subhedral zircons with ages clustering around ~2.0 Ga (Figure 16; Jacob et al., 1978; Kroner et al., 1991; Tack et al., 2002; Longridge, 2012; Foster et al., 2015; Longridge et al., 2018; Goslin, 2019). These grains reportedly display well-developed concentric

magmatic zoning and Th/U ratios predominantly >0.1, consistent with crystallization from a melt. Regression of magmatic domains yields upper intercept ages of ~2.0–2.1 Ga across multiple studies, recording a Paleoproterozoic magmatic zircon crystallization event that is internally coherent and reproducible.

CL textures also demonstrate substantial subsequent modification. Reported features include convolute and patchy zoning, homogenised domains, truncation of magmatic cores by bulbous embayments, ghost oscillatory zoning, pervasive fracturing, and metamictisation. Thin (<10 μm), bright rims and fracture-controlled overgrowths indicate new zircon growth during younger metamorphic events rather than simple Pb-loss. U–Pb datasets are commonly discordant and rely on regression to upper intercepts, with variable lower intercept ages and overlapping Th/U ratios between magmatic and metamorphic domains. Collectively, these features indicate that the zircon system experienced recrystallization, dissolution–reprecipitation, and partial isotopic disturbance during later thermal events.

The zircon record therefore demonstrates the presence of Paleoproterozoic magmatic zircon and its subsequent reworking. However, zircon ages and textures alone cannot distinguish whether the present host rocks crystallized as coherent granitoid bodies at ~2.0 Ga and were later preserved as an intact basement block, or whether Paleoproterozoic zircon was eroded from older crust, incorporated into Neoproterozoic sedimentary sequences, inverted during collision, and subsequently migmatised during high-temperature metamorphism and partial melting in the Damara Orogeny. Distinguishing between these scenarios is dependent on the surrounding field relationships and tectonic context.

Field relationships in the Ida Dome and Husabberg Anticlinorium indicate that granites and migmatites of the Abbabis Complex intrude and cross-cut the overlying Damara Supergroup (Figure 8D, 14 & 15), and that metasedimentary units resembling those of the Damara Supergroup are preserved as rafts and laterally continuous horizons within the migmatites of the Abbabis Complex (Section 3.1.3). In the absence of a distinct stratigraphic or depositional horizon, combined with the identical zircon ages in the Nosib Group of the Damara Supergroup (Figure 16), the presence of ~1–2 Ga zircon populations in the Abbabis Complex could be explained as inheritance from metasedimentary protolith rocks to the migmatites. Our field mapping could not confirm the existence of an unconformably older basement terrane amongst the volumetrically dominant Damaran-aged leucogranites and migmatites; an unconformably older basement terrane is not required to account for the existence of ~1-2 Ga zircon grains within the migmatites.

A further limitation of existing zircon geochronology studies is that zircon was separated from whole-rock gneisses rather than from physically isolated leucosome domains. Field relations presented

here indicate that the granitic gneisses of the Abbabis Complex in the Ida Dome and Husabberg Anticlinorium are migmatitic in character. Migmatites comprise remnants of older protolith preserved in the melanosome together with newly formed granitic material in the leucosome. Xenocrystic zircon commonly survives partial melting within the melanosome (Williams, 2001; Yakymchuk and Brown, 2014), meaning that whole-rock zircon populations in migmatites cannot be assumed to date melt generation or melt transfer. It is therefore not possible to compare the absolute age of the granitic leucosome in the Abbabis Complex to the age of leucogranite dykes intruding into the overlying Damara Supergroup, and we rely instead on well-exposed field (Section 3.1 to 3.4) and geochemical (Section 3.6) relationships.

4.6 Future work

Further investigation of the work presented here involves:

i. Geochronology which specifically separates the leucosome from the melanosome in Abbabis Complex migmatites. This may help separate magmatic zircon ages from xenocrystic zircon grains, thereby further constraining the relationship of leucosomes in the Abbabis Complex to leucogranite dykes intruding into the overlying Damara Supergroup.

ii. Systematic geochronology of the more massive leucogranite accumulations occurring as dykes and pluton-like bodies amongst the Abbabis Complex (Figure 11 & 12). This could confirm that larger leucogranite accumulations occurring amongst the Abbabis Complex are part of the same interconnected magmatic system as both the migmatites and the leucogranite dykes which intrude into the overlying Damara Metasedimentary Supergroup, as is implied from the field and geochemical data presented here.

iii. Detailed mapping and analysis of the Abbabis Complex in the cores of other dome structures throughout the southern Central Zone. The results of this study are specific to the Ida Dome and Husabberg Anticlinonrium. It remains to be tested whether similar field relations exist in other dome structures throughout the region.

4.7 Regional Implications

Interpretation of the Abbabis Complex as a melt-dominated migmatite-granite system in the core of the Ida Dome and Husabberg Anticlinorium (Figure 22) raises questions over the nature of the Abbabis Complex elsewhere in the southern Central Zone. Similar geological descriptions have been given in all areas where the Abbabis is mapped previously; it consists of an older metasedimentary and metavolcanic suite cross-cut by a volumetrically more abundant orthogneisses, granitic gneisses, leucocratic augen gneisses and (in places) intrusive granites (Smith, 1965; Marlow, 1981; Barnes, 1981; Sawyer, 1979; Jacob et al., 1983; Brandt, 1987; Longridge, 2012). This warrants reinvestigation of the Abbabis Complex elsewhere to determine the extent of the melt-dominated system documented here.

Partial melting and granite intrusion have fundamental impacts on the structural and geodynamic evolution of orogenic belts. Experimental evidence suggests that small melt volumes (~7%) are sufficient for the 'melt connectivity transition' - a critical boundary where an increasingly interconnected melt film around grain boundaries causes an overwhelming reduction in the aggregate strength of rocks (Rosenberg and Handy, 2005). Partially molten mid-crustal domains can fundamentally change the geodynamic evolution of the orogen, limiting crustal thickening and leading to regional-scale ductile flow of the mid-crust in response to differential pressure gradients (Jamieson and Beaumont, 2013). Large-scale ductile flow is a key component of the 'Channel Flow' model suggested to account for ductile extrusion of high-grade metamorphic rocks in the Himalayan orogen (Beaumont et al., 2001; Godin et al., 2006). In the Damara Orogen, the complexity and diversity of dome-and-basin and fold interference structures in the southern Central Zone has intrigued geologists for decades (Barnes and Downing, 1979; Barnes, 1981; Kroner, 1984; Oliver, 1994, 1995; Poli and Oliver, 2001; Kisters et al., 2004; Longridge et al., 2011; Ormond et al., 2024). The structural complexity of the southern Central Zone differs notably from the simpler fold-and-thrust belts of the bounding Northern and Southern Zones (Hartnady, 2014; Meneghini et al., 2014; Lehman et al., 2016; Passchier et al., 2016; Kitt et al., 2018). Understanding the extent of the melt-dominated system documented here (Figure 22) in the cores of other domes throughout the southern Central Zone is critical to understanding what role melting and magmatism played in the structural and geodynamic evolution of the Damara Orogen.

Finally, the syn-orogenic melt-dominated system documented in the core of the Ida Dome and Husabberg Anticlinorium (Figure 22) has important implications for economic geology. World-class uranium deposits are hosted in leucogranite dykes which intrude into the Damara Supergroup on the limbs of km-scale dome structures in the southern Central Zone (Kinnaird and Nex, 2007). Field and

geochemical evidence presented in this study documents melt transport through an interconnected migmatite-granite system in the cores of dome structures, culminating in the intrusion of leucogranite dykes into overlying metasedimentary units on dome limbs (Figure 22). This provides important architectural and plumbing constraints for understanding the evolution of the leucogranite-hosted uranium mineral system.

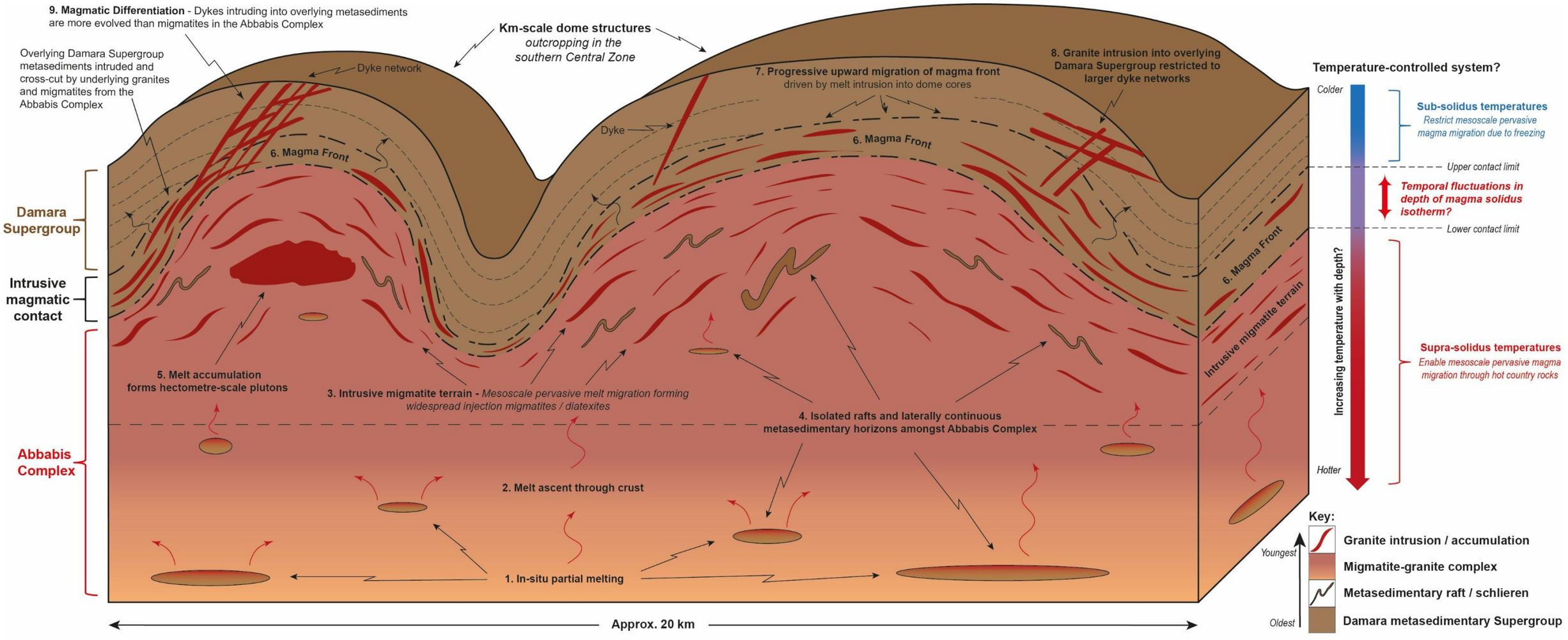

Figure 22 – Conceptual model for the formation and evolution of a mid-crustal migmatite-granite network as observed in the Ida Dome and Husabberg Anticlinorium. Upward migration of melt through the domes is associated with magmatic differentiation; dykes intruding into the overlying Damara Supergroup are relatively more evolved than the migmatitic leucosomes in the dome cores.

4. Conclusions

New field and geochemical data from the Ida Dome and Husabberg Anticlinorium prompts re-evaluation of the Abbabis Complex in the cores of these 2 dome structures. The principal conclusions of this study are:

1) ***Intrusive architecture of the contact:*** The boundary between the Abbabis Complex and the overlying Damara Supergroup is not defined by an angular unconformity, distinct stratigraphic break, or localized high-strain shear zone. Instead, it is characterized by a gradational intrusive transition in which migmatites and leucogranite bodies cross-cut and invade coherent overlying metasedimentary sequences. Domains mapped as "Abbabis Complex" correspond to volumetrically melt-dominated zones rather than to a discrete basement–cover boundary.

2) ***Melt connectivity and magmatic coherence***: Leucosomes within migmatites and leucogranite dykes intruding the Damara Supergroup display closely similar major and trace element compositions and consistent fractionation trends. Systematic geochemical differences indicate that dykes represent more evolved melts derived from the same magmatic system. These relationships support field evidence for an interconnected mid-crustal melt-transfer network.

3) ***Syn-orogenic formation during Damaran metamorphism***: Field relations, geochemistry, and regional metamorphic constraints are consistent with formation of a melt-dominated migmatite–granite complex during high-temperature Damaran metamorphism (peak at c. 520 Ma), involving partial melting of metasedimentary protoliths and upward melt migration.

4) ***Implications for zircon age interpretation***: Previously reported c. 1–2 Ga zircon age populations overlap with detrital zircon spectra from the Damara Supergroup; these could be explained as inherited xenocrystic zircon derived from metasedimentary protoliths to the migmatites in the Abbabis Copmlex; they do not necessarily require the existence of a pre-Damaran basement terrane. We outline how future geochronological work on migmatites and leucogranites of the Abbabis Complex could help further constrain their absolute timing relative to leucogranite magmatism in the overlying Damara Metasedimentary Supergroup.

Taken together, these observations indicate that the Abbabis Complex in the Ida Dome and Husabberg Anticlinorium records syn-orogenic crustal melting, melt migration, and accumulation within the mid-crust of the Damara Orogen. Recognition of this as predominantly melt-dominated architecture has

implications for the crustal structure, mineral system models, as well as the tectonic and geodynamic evolution of the Damara Orogen. However, the extent of these implications is dependent on whether similar field relationships are present in other areas previously mapped as the Abbabis Complex; the nature of the Abbabis Complex in other dome structures therefore warrants re-investigation.

6. ACKNOWLEDGMENTS

This work was undertaken as part of T. Jones' PhD research. The support of the DST-NRF Centre of Excellence for Integrated Mineral and Energy Resource Analysis (DST-NRF CIMERA) towards this research is hereby acknowledged. Additional support provided by the Society of Economic Geologists (SEG) in the form of a Graduate Student Fellowship and a Student Research Grant from the McKinstry Fund is greatly appreciated. Deep Yellow Ltd contributed towards the PhD funding of T. Jones and provided logistical support during fieldwork. Judith Kinnaird, Paul Nex and Roger Gibson are thanked for extensive discussion on this topic and earlier versions of the manuscript prior to submission. Opinions expressed and conclusions arrived at are solely those of the authors; they do not represent the opinions or conclusions of the supporting bodies or acknowledged individuals.

Appendix I : Description of element pair and ratio plots

Feldspar fractionation:

- ***Ba vs Sr*** plots track feldspar control on the system, since Ba is mostly partitioned into K-feldspar while Sr is partitioned into plagioclase.
- ***Rb/Sr vs Sr*** plots primarily track plagioclase control. Plagioclase crystallisation removes Sr, whereas Rb is highly incompatible and remains in the melt.
- ***Eu/Eu* vs Sr*** further tests plagioclase control. Both Eu and Sr substitute into plagioclase, meaning that Sr and Eu/Eu* typically produce a positive correlation as plagioclase crystallises.

Degree of differentiation:

- ***K/Rb vs Rb*** tests the degree of differentiation. Like K, Rb substitutes into K-feldspar and biotite. However, Rb is more incompatible than K, meaning that it is removed from the melt less efficiently. Differentiation therefore results in higher Rb concentrations and lower K/Rb ratios.

Accessory mineral control:

- ***Th vs La*** typically tracks accessory mineral control – especially monazite. Monazite crystallisation removes Th and LREE (for which La is a proxy) from the melt.
- ***Zr vs Hf*** tracks zircon. Since Zr and Hf are geochemical twins, they substitute into zircon near-identically. Under closed-system differentiation they maintain a near-constant ratio. Deviations imply different source signatures, inheritance, accumulation, contamination or different melt populations. Higher Zr-Hf values in a sample can reflect entrained/inherited zircon crystals, hotter melts which dissolved more zircon (zircon solubility in melt is strongly temperature dependent), or zircon crystallisation.
- ***Th vs Zr*** tracks the relationship between accessory phases monazite (Th control) and zircon (Zr control). Tight linear correlation suggests accessory phases behaved coherently, while scatter or decoupling can imply independent fractionation, different melting reactions, or source heterogeneity.
- ***Zr vs Y*** tests zircon behaviour against accessory minerals controlling HREE/Y-bearing phases. Y can be affected by retained garnet in the source, as well as xenotime and monazite.
- ***Ta vs Nb*** tracks high field strength element (HFSE) behaviour. Nb and Ta are geochemical twins which behave similarly and are mostly controlled by accessory phases such as rutile, ilmenite and titanite, as well as residual phases in the source.

- ***Nb/Ta vs Nb*** tests whether the Nb/Ta ratio changes as the system becomes more enriched in Nb. Changes in Nb/Ta ratio with Nb enrichment can indicate Ti-phase fractionation, source heterogeneity, or mixing between melts with different Nb/Ta ratios. Conversely, coherent behaviour implies no strong fractionation between Nb and Ta, no obvious rutile-controlled residual effect, and likely a similar source reservoir.
- ***Y vs Yb*** tracks HREE behaviour, and is often a check on garnet, xenotime and amphibole control. Tight positive linear trends indicate that HREEs are behaving coherently, with differences between populations mostly due to degree of enrichment or dilution rather than residual mineralogy. Decoupling, scatter, or multiple trends can conversely indicate garnet in the residue, xenotime or monazite affects, or mixing between melts.

8. REFERENCES CITED

Anders, E., Grevesse, N., 1989. Abundances of the elements: meteoric and solar. *Geochim. Cosmochim. Acta* **53**, 197–214.

Ashworth, L., Kinnaird, J.A., Nex, P.A.M., Harris, C., Müller, A., 2020. Origin of rare- element-mineralized Damara Belt pegmatites: a geochemical and light stable isotope study. *Lithos* **372–373**, 105655. https://doi.org/10.1016/j.lithos.2020.105655. ISSN: 0024-4937.

Barnes, J.F.H., 1981. Some aspects of the tectonic history of the Khan-Swakop region of the Damara Belt, Namibia. *Unpublished PhD thesis, University of Leeds, United Kingdom*.

Beaumont, C., Jamieson, R.A., Nguyen, M.H., Lee, B., 2001. Himalayan tectonics explained by extrusion of a low-viscosity crustal channel coupled to focused surface denudation. *Nature* **414**, 738 – 742.

Brandt, R. 1987. A revised stratigraphy for the Abbabis Complex in the Abbabis Inlier, Namibia. *South African Journal of Geology*. **90**, 314-323

Brown, M., 2007.Crustal melting and melt extraction, ascent and emplacement in orogens: Mechanisms and consequences. *Journal of the Geological Society* **164**, 709–730.

Brown, M., 2013. Granite: From genesis to emplacement. *Bulletin of the Geological Society of America* **125**, 1079–1113.

Corvino, A.F., Pretorius, L.E., 2013.Uraniferous leucogranites south of Ida Dome, central Damara Belt, Namibia: morphology, distribution and mineralisation. *Journal of African Earth Sciences* **80**, 60–73.

Cruden, A.R., Weinberg, R.G., 2018. Mechanisms of magma transport and storage in the lower and middle crust—magma segregation, ascent and emplacement. In: Burchardt (Ed.), Volcanic and Igneous Plumbing Systems Understanding Magma Transport, Storage, and Evolution in the Earth's Crust. *Elsevier*, pp. 13–53.

Fossen, H., Cavalcante, G. C. G., Pinheiro, R. V. L., & Archanjo, C. J. (2019). Deformation—Progressive or multiphase? *Journal of Structural Geology*, **125**, 82–99. https://doi.org/10.1016/j.jsg.2018.05.006

Foster, D.A., Goscombe, B.D., Newstead, B., Mapani, B., Mueller, P.A., Gregory, L.C., Muvangua, E., 2015, U-Pb age and Lu-Hf isotopic data of detrital zircons from the Neoproterozoic Damara Sequence: Implications for Congo and Kalahari before Gondwana, *Gondwana Research*, **28 (1)**, 179-190

Geological survey of Namibia 1995. Map Sheet 2214: Walvis Bay. *Geological Survey of Namibia, Windhoek*.

Godin, L., Grujic, D., Law, R.D., Searle, M.P., 2006. Channel flow, ductile extrusion and exhumation in continental collision zones: an introduction. *Geol. Soc. Spec. Publ.* **268**, 1–23. http://dx.doi.org/10.1144/GSL.SP.2006.268.01.01.

Goscombe, B., Foster, D. A., Gray, D., & Wade, B. 2017b. Metamorphic response and crustal architecture in a classical collisional orogen: The Damara Belt, Namibia. *Gondwana Research*, **52**, 80– 124. https://doi.org/10.1016/j.gr.2017.07.006

Goscombe, B., Foster, D.A., Gray, D., Wade, B., Marsellos, A., and Titus, J., 2017a. Deformation correlations, stress field switches and evolution of an orogenic intersection: The Pan-African Kaoko-Damara orogenic junction, Namibia: *Geoscience Frontiers*, **v. 8**, p. 1187–1232

Goslin, L.M., 2019. Deformation and partial melting in the Central Zone of the Damara Orogen, Namibia. *Unpublished Ph.D. thesis, University of the Witwatersrand*.

Gray, D.R., Foster, D.A., Goscombe, B., Passchier, C.W., Trouw, R.A.J., 2006. $^{40}Ar/^{39}Ar$ thermochronology of the Pan-African Damara Orogen, Namibia, with implications for tectonothermal and geodynamic evolution. *Precambrian Research* **150**, 49–72.

Gray, T., Kinnaird, J., Laberge, J., Caballero, A. 2021. Uraniferous leucogranites in the Rössing Area, Namibia: New insights from Geologic Mapping and Airborne Hyperspectral Imagery. Economic Geology. **116 (6)**, 1409-1434

Hartnady, M.I.H. 2014. The structural evolution of an ancient accretionary prism in the Damara Belt, Namibia. *Unpublished MSc thesis, University of Cape Town, South Africa*.

Hoffmann, K.-H., Condon, D. J., Bowring, S.A.& Crowley, J. L. 2004. U–Pb date from the Neoproterozoic Ghaub Formation, Namibia: Constraints on Marinoan glaciation. *Geology*, **29**, 1091–1094.

Jacob, R.E., 1974. Geology and metamorphic petrology of part of the Damara orogen along the lower Swakop river, South West Africa. *Unpublished PhD thesis, University of Cape Town, South Africa*.

Jacob, R.E., Kröner, A. and Burger, A.J., 1978. Areal extent and first U-Pb age of the Pre-Damaran Abbabis complex in the central Damara belt of South West Africa (Namibia). *International Journal of Earth Sciences*, **67**, 706–718.

Jacob, R.E., Snowden, P.A., Bunting, F.J.L., 1983. Geology and Structural development of the Tumas basement dome and its cover rocks. In: Miller, R.McG. (Ed.), Evolution of the Damara Oroqen

of South West Africa/Namibia. *Geological Society of South Africa, Special Publication* **11**, pp. 409-421.

Jamieson, R. A., and C. Beaumont (2013), On the origin of orogens, *Geological Society of America Bulletin*. **125 (11-12)**, 1671–1702

Jones, T.L. 2026. Structural setting of U-bearing pegmatite mineralisation in the Damara Orogen, Namibia. *Ore Geology Reviews – manuscript in review*.

Jung, S., Brandt, S., Bast, R., Scherer, E.E., Berndt, J., 2019. Metamorphic petrology of a high-T/low-P granulite terrane (Damara belt, Namibia) – constraints from pseudosection modelling and high-precision Lu-Hf garnet-whole rock dating. *Journal of Metamorphic Geology*. **37 (1)**, 41–69. https://doi.org/10.1111/jmg.2019.37.issue- 110.1111/jmg.12448.

Jung, S., Hoernes, S., Mezger, K., 2001. Trace element and isotopic (Sr, Nd, Pb, O) arguments for a mid-crustal origin of Pan-African garnet-bearing S-type granites from the Damara orogen (Namibia). *Precambrian Research*. **110 (1)**, 325–355. https://doi. org/10.1016/S0301-9268(01)00175-9.

Kinnaird, J.A., Nex, P.A.M., 2007. A review of geological controls on uranium mineralisation in sheeted leucogranites within the Damara Orogen, Namibia. *Trans I.M.M. Applied Earth Sciences* **116(2)**, 68-85.

Kisters, A.F.M., Ward, R.A., Anthonissen, C.J., Vietze, M.E., 2009, Melt segregation and far-field melt transfer in the mid-crust, *Journal of the Geological Society*, **166 (5)**, 905-918

Kitt, S., A. Kisters, I. Buick, and J. Kramers. 2018. Structural, Geochronological and P-T Constraints on Subduction-Accretion Processes in a Pan-African Accretionary Wedge—The Deep Level Southern Zone of the Damara Belt in Namibia. *Precambrian Research* **310**: 39–62.

Knupp, K.P. 2019. Regional Airborne Geophysical Interpretation, Uranium Province, Western Namibia. *Internal report produced on behalf of Reptile Mineral Resources, Swakopmund, Namibia*.

Kroner, A. (1984), Dome structures and basement reactivation in the Pan-African Damara belt of Namibia, in Precambrian Tectonics Illustrated, edited by A. Kroner and R. Greiling, pp. 191 – 206, *E. Schweizerbart'sche, Stuttgart, Germany*.

Kroner, A., Retief, E. A., Compston, W., Jacob, R. E. & Burger, A. J. 1991. Single-grain and conventional zircon dating of remobilized basement gneisses in the central Damara belt of Namibia. *South African Journal of Geology*, **94**, 379-387.

Kruger, T., Kisters, A., 2016. Magma accumulation and segregation during regional-scale folding: the Holland's dome granite injection complex, Damara belt, Namibia. *Journal of Structural Geology* http://dx.doi.org/10.1016/j.jsg.2016.05.002.

Lehmann, J., Saalmann, K., Naydenov, K.V., Milani, L., Belyanin, G.A., Zwingmann, H., Charlesworth, G., Kinnaird, J.A., 2016. Structural and geochronological constraints on the Pan-African tectonic evolution of the northern Damara Belt, Namibia. *Tectonics* **35 (1)**, 103135.

Lehtonen, M.I., Manninen, T.E.T., Schreiber, U.M., 1996, Report: Lithostratigraphy of the area between the Swakop, Khan and lower Omaruru Rivers, Namib Desert. *Communications of the Geological Survey of Namibia*, **11**, 71-82

Leitch, A.M., and Weinberg, R.F., 2002, Modelling granite migration by mesoscale pervasive flow: *Earth and Planetary Science Letters*, v. **200**, p. 131–146, doi:10.1016 /S0012-821X(02)00596-4.

Longridge, L., 2012. Tectonothermal Evolution of the Southwestern Central Zone, Damara Belt, Namibia. *Unpublished Ph.D. thesis, University of the Witwatersrand, South Africa* (522 pp.).

Longridge, L., Gibson, R.L., Kinnaird, J.A. and Armstrong, R.A., 2011. Constraining the timing of deformation in the southwestern Central Zone of the Damara Belt, Namibia. In: D.J.J. Van Hinsbergen, S.J.H. Buiter, T.H. Torsvik, C. Gaina and S.J. Webb (Editors), The Formation and Evolution of Africa: A Synopsis of 3.8 Ga of Earth History. *Geological Society, London, Special Publications*, **357**, 107–135.

Longridge, L., Gibson, R.L., Kinnaird, J.A. and Armstrong, R.A., 2017. New constraints on the age and conditions of LPHT metamorphism in the southwestern Central Zone of the Damara Belt, Namibia and implications for tectonic setting. *Lithos* , 278-281, 361–382. doi: 10.1016/j.lithos.2017.02.006

Longridge, L., Kinnaird, J.A., Gibson, R., Hawkesworth, C., Armstrong, R., 2018.Crystal recycling in the Damara Belt, Namibia, and interaction of the Congo and KalahariCratons–evidence from zircon U–Pb, Hf and O isotopes. *South African Journal of Geology*. **121 (3)**,237–252.

MacRoberts, R.J. 2025. Polyphase deformation during prolonged high-temperature, low-pressure metamorphism: An example from the Namibfontein-Vergenoeg migmatite domes, Central Zone, Damara Belt, Namibia. *Journal of Metamorphic Geology*. **0**. 1-35.

Marlow, A.G., 1981. Remobilisation and primary uranium genesis in the Damaran Orogenic Belt, Namibia. *Unpublished PhD thesis, University of Leeds, United Kingdom*.

Meneghini, F., A. Kisters, I. Buick, and Å. Fagereng (2014), Fingerprints of late Neoproterozoic ridge subduction in the Pan–African Damara belt, Namibia, *Geology*, doi:10.1130/g35932.1.

Miller R. McG., 2008. The geology of Namibia, Vol. 2: Neoproterozoic to Lower Paleocene. *Geol. Survey Namibia, Windhoek. Namibia*.

Miller, R. McG. & Grote, W. 1988. Geological Map of the Damara orogen, Namibia (scale 1:500,000). *Geological Survey of Namibia, Windhoek*.

Oliver, G.J.H., 1994. Mid-crustal detachment and domes in the central zone of the Damara orogen Namibia. *Journal of African Earth Sciences* **19**, 331–344.

Oliver, G.J. 1995. The Central zone of the Damara orogen, Namibia, as a deep metamorphic core complex. *Communications of the Geological Survey of Namibia*, **10**, 33-41.

Passchier CW, Trouw R, Schmitt RS (2016) How to make a transverse triple junction—new evidence for the assemblage of Gondwana along the Kaoko-Damara belts, Namibia. *Geology* **44(10)**:843–846. https://doi.org/10.1130/G38015.1

Paul, A., S. Jung, R. L. Romer, A. Stracke, and F. Hauff (2014), Petrogenesis of synorogenic high-temperature leucogranites (Damara orogen, Namibia): Constraints from U–Pb monazite ages and Nd, Sr and Pb isotopes, *Gondwana Research*, **25(4)**, 1614–1626, doi:10.1016/j.gr.2013.06.008.

Rosenberg, C.L., Handy, M.R., 2005. Experimental deformation of partially melted granite revisited: implications for the continental crust. *Journal of Metamorphic Geology*. **23**, 19–28.

Sawyer, E.W., 1979. The geology of an area south-east of Walvis Bay: *Lithology and field relationships, Rep. geol. Surv. S.W. Afr. (unpublished).*

Searle, M.P., Cottle, J.M., Streule, M.J. & Waters, D.J. 2009. Crustal melt granites and migmatites along the Himalaya: melt source, segregation, transport and granite emplacement mechanisms. *Transactions of the Royal Society of Edinburgh*, **100**, 219–233, doi:10.1017/S175569100901617X.

Smith, D.A.M., 1965. The geology of the area around the Khan and Swakop Rivers in SW Africa. *Geological Survey South Africa, Memoir 3*, 1-113.

Tack, L., Williams, I. and Bowden, P., 2002. SHRIMP constraints on early post-collisional granitoids of the Ida Dome, central Damara (Pan-African) Belt, western Namibia. *Abstracts of the 11th IAGOD Quadrennial Symposium and Geocongress, Windhoek, Namibia*.

Toé, W., Vanderhaeghe, O., André-Mayer, A.-S., Feybesse, J.-L., & Milési, J.-P. (2013). From migmatites to granites in the Pan-African Damara orogenic belt, Namibia. *Journal of African Earth Sciences*, **85**, 62–74. https://doi.org/10.1016/j.jafrearsci.2013.04.009

Ward R., Stevens G., Kisters A., 2008, Fluid and deformation induced partial melting and melt volumes in low-temperature granulite-facies metasediments, Damara Belt, Namibia: *Lithos* , v. **105**, p. 253–271, doi:10.1016/j.lithos.2008.04.001.

Weinberg, R.F., 1999, Mesoscale pervasive melt migration: Alternative to dyking: *Lithos*, v. **46**, p. 393–410, doi: 10.1016/S0024-4937(98)00075-9.

Weinberg, R.F., and Searle, M.P., 1998, The Pangong injection complex, Indian Karakoram: A case of pervasive granite flow through hot viscous crust: *Journal of the Geological Society of London*, v. **155**, p. 883–891, doi:10.1144/gsjgs.155.5.0883.

Williams, I. 2001. Response of detrital zircon and monazite, and their U–Pb isotopic systems, to regional metamorphism and host-rock partial melting, Cooma Complex, southeastern Australia. *Australian Journal of Earth Sciences*, **48**, 557–580.

Yakymchuk, C., & Brown, M. (2014). Behaviour of zircon and monazite during crustal melting. *Journal of the Geological Society*, **171**, 465–479. https://doi.org/10.1144/jgs2013-115